Macrophage Interactions with Decellularized Heart Valve Materials: Influence of Crosslinking Treatment

by

Jonathan Keith McDade

Submitted in partial fulfillment of the requirements
for the degree of Master of Applied Science

at

Dalhousie University
Halifax, Nova Scotia
August 2010

DALHOUSIE UNIVERSITY

SCHOOL OF BIOMEDICAL ENGINEERING

The undersigned hereby certify that they have read and recommended to the Faculty of Graduate Studies for acceptance a thesis entitled "Macrophage Interactions with Decellularized Heart Valve Materials: Influence of Crosslinking Treatment" by Jonathan Keith McDade in partial fulfillment of the requirements for the degree of Master of Applied Science

Dated: August 24th, 2010

Co-Supervisor: _____

Co-Supervisor: _____

Readers: _____

_____

DALHOUSIE UNIVERSITY

DATE: August 24, 2010

AUTHOR: Jonathan Keith McDade

TITLE: Macrophage Interactions with Decellularized Heart Valve Materials: Influence of Crosslinking Treatment

DEPARTMENT OR SCHOOL: School of Biomedical Engineering

DEGREE: MASc CONVOCATION: October YEAR: 2010

Permission is herewith granted to Dalhousie University to circulate and to have copied for non-commercial purposes, at its discretion, the above title upon request of individuals or institutions.

_____

Signature of Author

Dedicated to:

My late grandparents,

Bruce and Helen McDade

Table of Contents

List of Figures

List of Tables

Abstract

While macrophages have been implicated in the failure of bioprosthetic heart valves, there is no current literature on the macrophage response to crosslinked, native collagen. Using decellularized bovine pericardium (DBP) as a model, this study investigates the response of macrophage-like cells (U937s) to untreated DBP and DBP under two chemical crosslinking techniques: glutaraldehyde (GLUT) and an alternative zero-length crosslinker 1-ethyl-3-(3-dimethylaminopropyl)-carbodiimide (EDC). U937 cells were seeded and differentiated directly on the material surfaces. At 72 h after differentiation, the samples were fixed for SEM as well as analyzed for acid phosphatase activity, cytokine and matrix metalloproteinase release, all normalized to the number of live, adherent cells via DNA analysis. The U937 cells on the GLUT surface showed an abnormal morphology not seen on the other surfaces. These cells released more pro-inflammatory cytokines, and less MMP-2 and MMP-9 than occurred under EDC treatment or in untreated DBP. The results suggest that host inflammatory cells react to the crosslinking state of the DBP, perhaps as a non-specific response.

List of Abbreviations and Symbols Used

ANOVA	analysis of variance
DBP	decellularized bovine pericardium
DNAse	deoxyribonuclease
DSC	differential scanning calorimetry
ECM	extracellular matrix
EDC	1-ethyl-3-(3-dimethylaminopropyl) carbodiimide hydrochloride
EDTA	ethylene diamine tetraacetic acid
ELISA	enzyme-linked immunosorbent assay
FBGC	foreign body giant cells
IL-1Ra	interleukin-1 receptor antagonist
IL-6	interleukin-6
IL-10	interleukin-10
LDH	lactic acid dehydrogenase
M	molar (mole/L)
MDM	monocyte-derived macrophages
MMP	matrix metalloproteinase
NHS	N-hydroxysuccinimide
nM	nanomolar
nmol	nanomole
PBS	phosphate buffered saline
PMA	phorbol 12-myristate 13-acetate
PMN	polymorphonuclear cells, neutrophils
PMSF	phenylmethylsulfonyl fluoride
RNAse	ribonuclease
SD	standard deviation
SE	standard error of the mean
SEM	scanning electron microscopy
TCPS	tissue culture polystyrene
TNF-α	tumor necrosis factor-alpha
U	units

Acknowledgements

So many people have shaped my graduate school experience. I would like to begin by thanking my co-supervisors Dr. Michael Lee and Dr. Rosalind Labow, for taking me under their guidance and making my research possible. Thanks to their mentorship for the past two years, I have learned so much about research in general and tissue mechanics in particular. I would also like to thank my excellent committee members Dr. Paul Gratzer and Dr. Sarah Wells for sharing their great ideas and feedback with me.

I would like to thank everyone that has been a part of the Tissue Mechanics Lab Group over the past two years for being such a great group of people to work with. In particular, I thank Dr. Marianne Ariganello for all the great advice and experience you have given me. It has been a pleasure working with you, from the humble beginning to the end, you have been an outstanding wealth of knowledge. Thanks to Dr. Ellen Brennan for all her support, and help with the follow-up studies complimenting the work done in this thesis. I would like to thank Dr. Ping Li for his critical point drying and sputter coating services for SEM, and Patricia Scallion for all the training and assistance with the SEM. Thanks to Michel Johnson for his guidance with the differential scanning calorimetry experiments. I would like to thank everyone at OH Armstrong Food Services in Kingston NS for the bovine pericardium used throughout this thesis. A very special thanks to Sandy Mansfield for everything she has done over the past two years and all the conversations we had every time I would walk by her office. I would like to thank Maxine Langman for all her techni-

cal and experimental training. I would like to acknowledge the support of the Canada Foundation for Innovation, the Atlantic Innovation Fund, and other partners which fund the Facilities for Materials Characterization, managed by the Institute for the Research in Materials. I would also like to thank the Natural Sciences and Engineering Research Council (NSERC) for providing operating funds and personal stipend for this work.

I want to thank my amazing family and friends for all of their support. I am so grateful for my beautiful wife, Jizelle, who has been a bottomless source of happiness, love and support. Finally, I would not be where I am today without my family, Drew, Nancy, and Emily McDade. I am very grateful for their life-long love, support and unwavering confidence in me.

Chapter 1: Introduction

1.1 Background

Natural heart valves open and close over 35 million times each year. When natural heart valves fail due to disease-induced obstruction or leaks, they must be replaced to improve the life expectancy of the patient. Bioprosthetic heart valves derived from natural tissues, including porcine aortic valves and bovine pericardium (the sac that contains the heart and the roots of the great vessels), have gained wide acceptance as an appropriate replacement for failing natural valves. However, the ability of bioprostheses to withstand continuous cyclic loading and attack from biological factors, without any capabilities to renew or replace damaged tissue components, continues to be a major concern.

Every year, 290,000 patients globally are diagnosed with a pathological valve that cannot be repaired and must be replaced[1]. Presently, heart valve replacement surgery is the most common form of therapy for late-stage heart valve disease[2]. In most instances, diseased valves are replaced with either completely synthetic mechanical valves or bioprosthetic valves derived from either porcine aortic valves or bovine pericardial tissue, crosslinked with glutaraldehyde. Unlike mechanical valves which are very durable, bioprosthetic valves suffer from limited long-term performance attributed to both calcification and primary tissue failure stemming from material fatigue[2-6]. As of 1999, despite these durability issues, tissue-derived valves are used in over 40% of replacement surgeries in North America because of (i) their central blood flow characteristic which minimizes hemolysis and (ii) the valve recipi-

ent's freedom from anticoagulation therapy upon implantation[7]. However, until the mechanisms involved in the development of primary tissue failure are completely understood and overcome, the uncertain functional life-span of glutaraldehyde-crosslinked bioprosthetic valves will inevitably limit their use especially in younger patients[8].

Explant studies of failed tissue-valve replacements revealed either mechanical disruption of the leaflet, host cell infiltration, or both. The primary cell type identified was generally described as host macrophages[9]. Nonetheless, the factors that plague bioprosthetic heart valves, such as high re-operation rate as a result of poor durability, persist[10].

In the past decade, tissue valve replacement design has shifted towards materials that have the potential for remodeling; however, these materials are even less understood in terms of long-term performance and host cell interaction. The objective of this thesis was to probe the interaction of macrophages with decellularized bovine pericardium (a current biomaterial used as a prototype matrix for new generation heart valve replacements) and to look at the effect of matrix crosslinking in the absence of other factors such as blood serum, blood cells, and cellular debris from xenogenic sources with different chemical agents in an attempt to gain further understanding of tissue-derived valve failure.

1.2 Heart Valve Replacement

The four valves of the human heart are exposed to a complex biological and mechanical environment. Each year, these collagen-based tissues must withstand fatigue loading associated with opening and closing while interacting with blood cells, protein, and plasma under high flow, and must perform ongoing repair of any damage[11]. Due to the vital function of heart valves in the body, a malfunction or defect must be repaired quickly as a deficiency of these valves can lead to heart failure and subsequent death.

The gold standard for tissue valve replacement uses allograft valves from cadavers that are antibiotic-treated and cryopreserved[12]. These valves, become progressively acellular in the patient and suffer from problems similar to any transplanted tissue: the possibility of an immune response leading to transplant tissue damage. This is especially troublesome in children, as there is limited availability of cadaveric valves and a difficulty in size matching the donated valve to the patients[13,14]. In addition, allograft valves typically last only 20 – 25 years within a patient, before the valve must be replaced due to inadequate performance[15,16].

Considering the multifaceted environment in which a native valve must function, the design of a high-functioning, long-lasting substitute valve is challenging. Currently, no clinically available valve replacement completely replicates the performance, function, and remodeling capability of a native valve[17]. None of the present valve replacements are ideal for young children as the primary concern clinically is calcification. Primary tissue degeneration due to calcification resulted in re-

operation or death in 20-25% of adult recipients of porcine aortic bioprotheses by 7-10 years after operation and in over 50% of children after a comparable period[18]. None of these current replacements are repopulated *in vivo* with appropriate host cells with each type of substitute valve having its own specific limitations.

1.2.1 Current Tissue Based Valves

The development of bioprosthetic valves came as an attempt to resolve the limited supply of allograft valves. Historically, bioprosthetic valves have been derived from either porcine aortic valves or bovine pericardium, although alternative animal sources have been explored[17].

A major drawback to the available heart valve replacements is the lack of growth, repair and remodeling capabilities. Generally, there are three types of replacement heart valves that are available for clinical use: porcine xenograft valves, bovine pericardial valves, and allograft or homograft valves. It has been reported that porcine aortic valves have a survival rate of 30% at 15 years in the mitral position[19], and that bovine pericardial valves have a survival rate of 37% at 14 years in the mitral position[20].

Pericardial bioprosthetic heart valves have been used successfully for many years[21]. Compared to porcine valves, they have better hydrodynamic and hemodynamic properties, although many patients receiving these prostheses require long-term anticoagulation or antiplatelet therapy. However, with most biological prostheses, their long-term function and durability can be affected by calcification. Initial

failures in the first generation of bovine pericardial bioprosthetic heart valves involved premature tearing due to poor design and construction, such as the suture attachment points of the valve cusps to the stent posts[22]. Early failure of the Ionescu-Shiley standard pericardial valve in the absence of calcification, has been extensively reported[21]. Glutaraldehyde was used to stabilize the collagen at 0 mm Hg transvalvular fixation pressure. The failures came from tears originating at the stitching, which penetrated the free margin of the leaflets and attached the pericardium to the stent posts, causing regurgitation[23].

The second generation bovine pericardial valves improved by removing the alignment suture, increasing durability with minimal design-related failures, when monitored over a 10-12 year post implantation period[20,24]. Nonetheless, this design did not address the complex configurational changes in the matrix structure inherent with glutaraldehyde crosslinking and subsequent calcification. The Carpentier-Edwards pericardial valve is currently available today as a porcine bioprosthetic valve alternative. This stented bovine pericardial prosthesis is glutaraldehyde-fixed and anti-calcification treated. The prosthesis has excellent durability in older patients but is subject to age-related structural deterioration[25]. The most common reason for valve explantation with the Carpentier-Edwards is failure due to intrinsic calcification, non-calcific degeneration, cusp bursting, cusp thickening or fibrosis, or a combination of these[25].

In order to minimize the immunological reaction that occurs when a xenogeneic, cellular tissue is placed into a human, bioprosthetic valves are crosslinked with

glutaraldehyde. The immunogenic 'protection' offered by glutaraldehyde fixation, although incomplete, eliminates the need for immunosuppression and its associated risks. This fixation, however, also results in a non-viable valve substitute with altered mechanical properties[11]. The crucial drawback of bioprosthetic valves is their poor long-term durability due to progressive structural deterioration over time[26]. Typically, 50% of bioprosthetic valves begin to fail within 12 – 15 years postoperatively, and this rate of structural failure is even greater in patients less than 35 years of age, especially children[11].

1.2.2 Failure of Bioprosthetic Heart Valves

Explant analysis of allografts and bioprostheses provides some illumination into the failure of implanted valves within the host, however the exact mechanisms of failure remain unclear. The primary observation in retrieved, failed tissue valves (excluding those that failed primarily due to calcification) was structural degeneration of the valve[7]. The collagen architecture was almost invariably modified in implanted heart valves, often with fluid or plasma insudation between adjacent collagen bundles[2] and/or the degeneration or fragmentation of collagen fibers[6,9]. As well, macrophages and/or inflammatory cells were a predominant cell type found on the surface of valves[27].

The clinical bioprosthetic valve failure due to tearing was often as a result of localized cuspal damage at or near the sites of highest stress, such as the commissures and points of maximal cuspal flexion (where the respective motions are non-

physiological)[5,28]. However, with finite element methods, solutions have been identified to reduce commissural stress, such as using flexible stent posts and reducing the angle between the horizontal top free edge of the leaflet and the vertical stent post[29,30]. Another mechanism of leaflet failure was initiated by abrasion of the pericardium against the cloth covered stent[28,31]. These abrasions occurred during diastole whenever the pericardium was mounted outside the stent post. With the pericardium mounted inside the post, the leaflet would not fail during diastole; however, it is possible to have abrasion during systole[32].

The contribution of non-calcific degeneration of bioprosthetic heart valve failure was first demonstrated by early work done through explant analysis by cardiovascular pathologists like Schoen *et al*.[2]. Even though calcification was present in a majority of the glutaraldehyde-treated bovine pericardial valves that were analyzed, cuspal defects occurred independent of these mineralized areas. More specifically, structural disruption of the collagen fibres and infiltration by inflammatory cells were observed frequently. Upon closer observation and analysis through hematoxylin and eosin staining, the inflammatory cell type found lining the surface of the valve was identified as the macrophage. Another study analyzed explanted human allografts and similarly demonstrated the presence of macrophages in approximately 80% of the valves[33].

Attempting to analyze the contribution of inflammatory cells to the degeneration of porcine bioprostheses, Stein *et al*.[34] utilized scanning electron microscopy and revealed that leukocytes were present on the surface of 82% of the valves explanted.

Again, macrophages were the most prevalent cell type, although neutrophils and lymphocytes were present in significant numbers as. Work by Grabenwöger *et al*.[9] showed similar results of apparent macrophage interaction with collagen fibers from bioprostheses.

The visualization of macrophages on the valvular surfaces of these biomaterials provides evidence of their presence, but does not explain how they were recruited or their specific function at the site. Nevertheless, early work by Simionescu *et al*.[35] supplies additional circumstantial evidence of the macrophage role in bioprosthetic valve degradation. Analysis of explanted, glutaraldehyde treated bovine pericardial valves revealed the presence of matrix-degrading enzymes in the tissues, suggesting that the bioprostheses were subject to enzymatic degradation[36]. More specifically, the enzymes found in the explanted tissues displayed matrix metalloproteinase (MMP) activity[37]. MMPs are a group of more than 23 calcium-dependent proteases that are capable of degrading most extracellular matrix (ECM) components and thus play an important role in tissue remodeling and repair[38]. Within this protein family, MMP-2 and MMP-9 have the ability to digest denatured collagen, or gelatin, and are referred to as gelatinases. The presence of these enzymes is evident when their activities in explanted valves are compared to that in freshly preserved, glutaraldehyde treated valves. The level of MMP-2 activity remained relatively constant in both groups whereas the level of MMP-9 activity was elevated at explantation[37]. Simionescu hypothesized that the bioprosthetic valve elicits a foreign body response that recruits phagocytic cells into the tissues. Following this, the activated

macrophages can secrete MMP-9, which begins the structural degeneration of the valvular tissue[37]. While this hypothesis is intriguing, a study by Ariganello *et al*.[39] demonstrated that cells will produce MMPs or matrix-degrading enzymes even when exposed to synthetic materials such as polystyrene and polydimethylsiloxane (PDMS).

1.2.3 Limitations of Current Explant Studies

While analysis of explanted valve tissues provides an indication of what occurs to the valves in the host, the exact mechanism(s) of failure cannot be conclusively elucidated. Any observations made from explant analysis must be made cautiously since the explants are not taken from a representative population of patients but rather are always obtained from patients who have experienced an undesired clinical outcome. Explant findings only highlight bio-incompatibility. Observations on the long term natural history of well-functioning valve replacements in humans are difficult to find.

As an example, it is still unclear whether macrophages are present on only failed valves or if they commonly interact with implanted functional valves. More importantly, explant studies only represent a single instant in time, which is failure. Any hypotheses regarding the mechanisms leading to failure, therefore, must be tested and viewed with caution. Adding to the aforementioned point, if there is a tear in the tissue and cells are observed surrounding the tear, it cannot be determined whether the cells caused the disruption in the tissue, if the tear released any

factors that may have recruited the cells to the site, or if there was a third factor that relates the two observations.

1.2.4 Decellularized Matrices and Bioprosthetic Heart Valves

With the advancements in the field of tissue engineering and regenerative medicine, the main focus has been on the *in vitro* generation of functional, living heart valve bioprostheses. The basic approach is through the use of starter matrices of polymers, both synthetic and naturally derived (pure collagen, collagen and proteoglycans), or decellularized xenogeneic as well as allogeneic materials configured to the appropriate shape of native heart valves.

A decellularized scaffold is created from freshly excised tissue that is chemically or physically treated to remove the cellular components in a controlled manner such that the structure and physical properties of the remaining original tissue are retained[40-42]. These scaffolds provide a three-dimensional architecture for cell interaction and may retain intrinsic adhesion and migration sites for cell attachment and growth because the collagenous structure remains in its native form[14]. Due to the highly conserved sequence of amino acids in collagen across species, the immunological response to decellularized connective tissue scaffolds should be mild, although conclusive human immunological studies of bovine and porcine collagen with intact non-helical ends are lacking[43,44]. However, due to the vascular location of a heart valve, it is also important to recognize that collagen is considered to be

thrombogenic[45] and that circulating platelets are not exposed to type I and III collagen except with tissue injury.

The current processing of both allogeneic and xenogeneic valve substitutes (antibiotic soaking with cryopreservation or crosslinking, respectively) is not sufficient to remove all immune responses. Patients who have received either valve type show antibodies that are reactive to the valve materials[46,47]. However, the process of crosslinking with glutaraldehyde does not remove the xenogeneic cells within the tissue; rather the crosslinks purportedly mask the antigenic components of those cells and make the cells non-viable[36].

1.3 Crosslinking Bioprosthetic Heart Valves

Glutaraldehyde-crosslinked bioprosthetic heart valves are widely used as replacement heart valves because of their low thrombogenicity. However, disappointing long-term durability stemming from structural fatigue and calcification limits their use, especially in younger patients[8]. Glutaraldehyde treatment itself has been implicated as a major contributor to these failure mechanisms, perhaps initiating the formation of calcification[2]. Glutaraldehyde crosslinking also increases the tissue's bending stiffness[48], resulting in premature valve failure due to repetitive flexing motion[49]. Moreover, glutaraldehyde elicits a cytotoxic reaction through the depolymerization of glutaraldehyde and the release of unreacted monomer into the surrounding tissue[50]. Prior research has also suggested there is a non-uniform crosslink density through the thickness of collagen bundles and fibers within pericardial tissue, leav-

ing the interior of the fibers or fibrils uncrosslinked[51]. In an attempt to alleviate these problems inherent with glutaraldehyde-crosslinking, alternate crosslinking methods are presently under investigation.

1.3.1 Crosslinking with Glutaraldehyde

The objective of pre-implant crosslinking has been to: (i) reduce immunogenetic reactions between tissue and host, (ii) sterilize the tissue, (iii) increase resistance to enzymatic degradation, and (iv) increase the long-term durability. Glutaraldehyde fixation of bioprosthetic heart valve materials is presently the industrial standard for chemical pretreatment of tissue-based bioprosthetic heart valves. Briefly, crosslinking occurs through the reaction of the aldehyde groups at either end of the glutaraldehyde molecule and the ε-amino groups of lysine or hydroxylysine residues within or between collagen molecules[51]. During treatment with glutaraldehyde, the cell layer is stripped and all interstitial cells are devitalized. Therefore crosslinking with glutaraldehyde leaves the tissue without a renewal mechanism to replace damaged tissue components[37].

1.3.2 Biochemistry of Glutaraldehyde Crosslinks

Glutaraldehyde is a water soluble, five-carbon dialdehyde molecule. Aqueous solutions of glutaraldehyde are complex mixtures of free aldehyde, mono and dihydrated monomeric glutaraldehyde, monomeric and polymeric cyclic hemiacetals and various α- and β-unsaturated polymers[52]. Crosslinking between glutaraldehyde

and bovine pericardium results in intramolecular and intermolecular covalent bonds (Figure 1-1).

The mechanism by which glutaraldehyde reacts with collagen is complex and not completely understood. Generally, glutaraldehyde crosslinking involves the initial formation of Schiff base intermediates, created by the nucleophillic attack between glutaraldehyde (slightly positive carbonyl carbon) and lysine or hydroxylysine (ε-amino groups)[53].

Parameters important in tissue stabilization using glutaraldehyde fixation include: glutaraldehyde concentration, stress state during fixation, time of exposure, temperature, pH, and the composition of the glutaraldehyde solution[52]. Fixation occurs rapidly and within one hour at a concentration of 0.5% glutaraldehyde at room temperature and a neutral pH, the reaction was 84% complete as measured by tissue thermal stability[52]. The reaction continues for over 24 hours, even though the crosslink density reaches equilibrium after a few hours. This may be due to changes in the nature of the crosslinks, possibly due to continued polymerization[52]. The use of lower concentrations of glutaraldehyde during fixation of the tissue slows the time-dependent crosslinking process, possibly reducing the effects of crosslinking on the surface of the collagen fibers[52]. Cheung and Nimni showed that at low concentrations of glutaraldehyde, intermolecular crosslinks were formed which prevented the tissue from being solubilized by cyanogen bromide (CNBr), but not by collagenase[51]. As the glutaraldehyde concentration increased, a more rapid crosslinking process was evident and the tissue became more resistant to

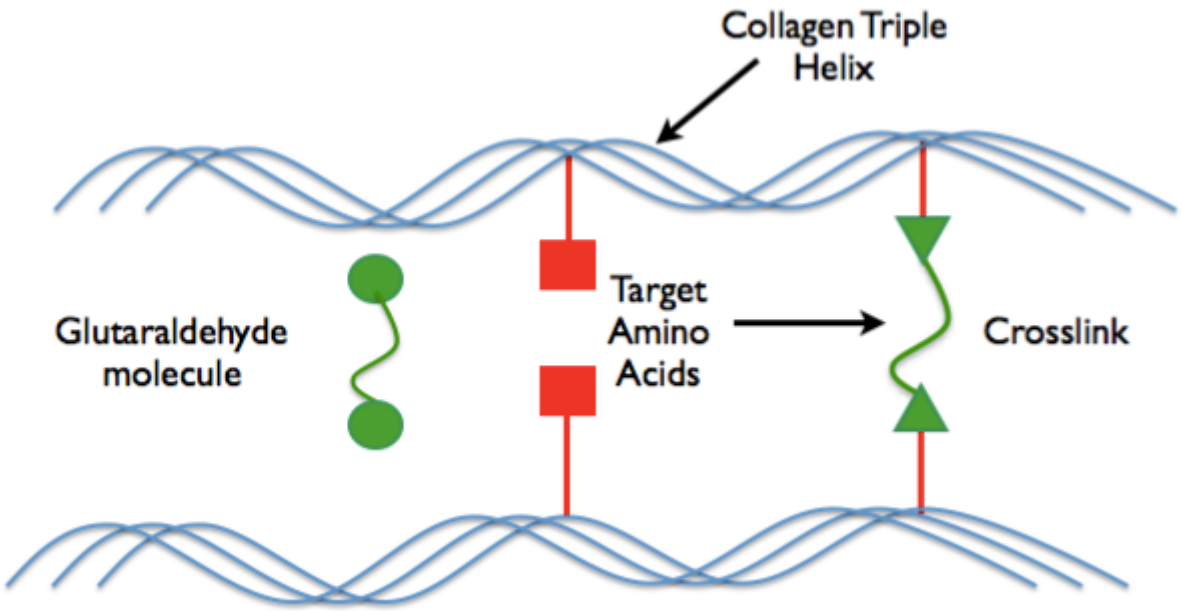

Figure 1-1: Glutaraldehyde forming an intermolecular collagen crosslink.
Interaction of the glutaraldehyde molecule with the target amino acids lysine and hydroxylysine in collagen. In this intermolecular crosslink, the glutaraldehyde molecule is consumed to form the linkage between the amino acid side groups.

collagenase[51,52]. However, there was only a small increase in the number of lysyl residues modified, reflecting an increase in the molecular length of glutaraldehyde polymers rather than an increase in the actual number of crosslinking sites[51].

Researchers have argued that glutaraldehyde acts only on the surface of dense collagenous tissue such as bovine pericardium, rather than penetrating into the interior of the tissue, resulting in an uneven distribution of glutaraldehyde crosslinks across the tissue's full thickness[51,53,54]. Fisher et al.[21] could not detect a variation in shrinkage temperature through different sections of bovine pericardial tissue crosslinked with glutaraldehyde, which suggested uniform penetration of the fixative and crosslinking. Also, Fisher et al.[21] could not determine whether the crosslinking took place at the surface of the collagen fibrils or penetrated deeper into the molecular structure. It has also been demonstrated that glutaraldehyde treated tissues were more susceptible to enzymatic digestion after denaturation when the inner, evidently less crosslinked molecules of the fibre were exposed to enzymes by hydrothermal denaturation[55]. This further supports the argument that incomplete or non-homogeneous fixation may play a role in mechanically fatigued tissues. Fatigue damage may expose inner, inadequately crosslinked collagen fibers which are then more susceptible to enzymatic degradation.

1.3.3 Crosslinking with Carbodiimide

To overcome the problem of reagent depolymerization and release of monomers, alternative crosslinking methods have been devised. These activating agents interact with carboxylic acid groups of glutamic or aspartic residues within the collagen molecule, making them reactive with lysyl amino groups, without the creation of a crosslinking bridge[54,56,57]. Weadock *et al.* first described the development of crosslinks in pure collagen films using cyanamide, the simplest type of carbodiimide[58]. More recently, Petite *et al.*[59] used the related acyl azide activation method to form crosslinks within bovine pericardium, resulting in tissue with similar resistance to degradation by bacterial collagenase as glutaraldehyde-treated tissue. In addition, collagenous biomaterials crosslinked using the acyl azide method had a decreased tendency to calcify compared to glutaraldehyde-treated tissue[59]. However, this crosslinking method was more complicated than the standard glutaraldehyde crosslinking treatment, likely making it impractical in an industrial setting[49,57].

An alternative carbodiimide crosslinking treatment using 1-ethyl-3-(3-dimethylaminopropyl) carbodiimide hydrochloride (EDC) has shown promise as a crosslinking treatment for bioprosthetic heart valves. Previously, it has been used in many areas of research, including: collagen-based scaffold preparation for tissue regeneration[60-62], peptide synthesis[63], and crosslinking of hyaluronic acid[64]. To improve the crosslinking efficiency, N-hydroxysuccinimide (NHS) has been used to convert an unstable intermediate product into a more stable ester group which is then reactive with the lysyl amino groups, forming peptide linkages[65,66]. EDC-

treatment of collagen-based biomaterials at an optimal pH of 5.5 produced similar or higher denaturation temperatures than those seen in materials treated with glutaraldehyde[64]. Previous studies have also assessed the resistance of EDC-treated collagen-based biomaterials to enzymatic degradation, again with mostly positive results[54,56].

EDC was chosen as the alternative crosslinking treatment in this study due to its ability to form different types of crosslinks compared to glutaraldehyde. While glutaraldehyde forms crosslinks between ε-amino groups of lysine or hydroxylysine residues of collagen, the EDC-treatment forms peptide linkages through the activation of the carboxyl and amino moieties. In addition, EDC-treatment forms crosslinks within the collagen structure without being incorporated into the material (Figure 1-2)[64]. Moreover, unlike glutaraldehyde, EDC is not capable of polymerizing, possibly improving its penetration into the interior of the tissue structure[54]. Lee and co-workers (1996)[54] showed that after the helical structure of collagen was disrupted, EDC-treated bovine pericardium was more resistant to enzymatic degradation than was glutaraldehyde-crosslinked tissue. Thus, mechanical fatigue damage, which disrupts the collagen structure, may not so much accelerate the enzymatic degradation of EDC-treated tissue—improving the long-term durability of bioprosthetic heart valves. Despite being a potential alternative for glutaraldehyde-fixation, commercial surgical products have not been crosslinked with EDC.

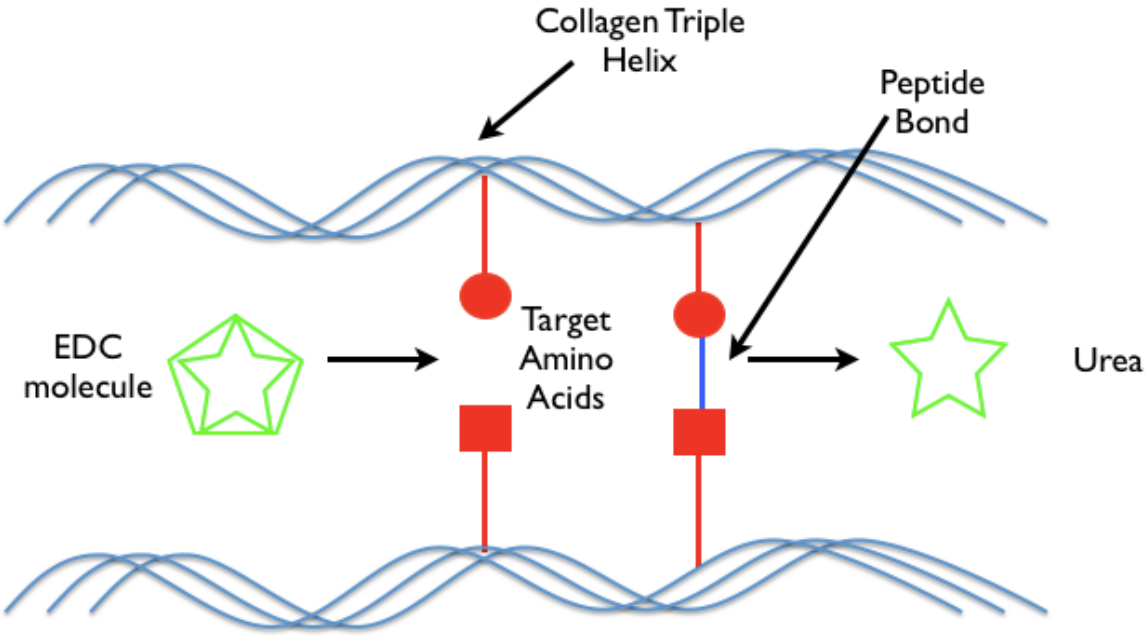

Figure 1-2: Carbodiimide forming a peptide crosslink in collagen.
Interaction of the carbodiimide molecule with the carboxy and amino terminals of the target amino acids in collagen. The carbodiimide molecule forms a peptide bond between the amino acids. In the reaction, the carbodiimide does not remain within the linkage but rather is consumed. The spent reagent is non-toxic to the cells and may be rinsed away.

1.4 Role of Macrophages in Bioprosthetic Heart Valves

1.4.1 Macrophage Recruitment and Function at the Biomaterial Implant Site

When a biomaterial is implanted into the host, an innate immune response (or foreign body reaction) occurs as a result of the injury to the tissue[67]. In response to this injury, local cells in the circulation such as mast cells and macrophages release cytokines and chemokines that affect local vasculature and cause recruitment of cells to the site of the injury[68,69]. More specifically, vessels nearby become more permeable and dilate allowing cells and signals within the vasculature to access the site more easily. By virtue of their numbers the cell type to respond first to the surgical implantation site are neutrophils (polymorphonuclear cells, PMNs) from peripheral blood vessels, which migrate through the vessel walls towards the inflammatory stimulus. Once at the site, PMNs will begin secreting additional chemokines to attract monocytes from the blood to begin migration through the tissue[70]. Differentiation from monocytes to macrophages then occurs on the biomaterial surface, which results in increases in cell size, protein synthesis, production of MMP-9, and changes to the cell surface receptors[71,72]. Once the monocytes have differentiated into macrophages, they begin to attach, spread along the surface, phagocytose debris, and secrete enzymes[67]. These monocyte-derived macrophages (MDMs) are terminally differentiated and do not multiply, therefore their accumulation at a wound or biomaterial site is due to the continuous recruitment of monocytes to that site[67]. Even though they

are terminally differentiated, cellular fusion can occur to form multi-nucleated cells that can further develop into foreign body giant cells (FBGCs)[71].

MDMs and FBGCs are recognized as the most abundant white cell type found on medical devices and the primary cells involved in the degradation and subsequent failure of many biomaterials[73-76]. The specific degradative capabilities of MDMs and FBGCs are directly related to the secretion of certain enzymes such as MMPs and lysosomal acid phosphatase[77]. Knowing this, it would be expected that MDMs play an explicit role in the failure of bioprosthetic heart valves.

The role of MDMs at the biomaterial implant site can be separated into two broad but connected functions: promoting inflammation and opposing inflammation (or wound healing)[69,78]. Further detailed descriptions of these two macrophage functions (or polarizations) have been discussed elsewhere and are referred to as classical versus alternative activation, and M1 versus M2 polarizations[79-81].

1.4.2 Pro-Inflammatory (M1) Polarization

The evolutionary role of MDMs at the site of inflammation is to identify foreign pathogens, primarily through scavenger receptors or complement receptors and to ingest or degrade these potentially dangerous materials[82]. The majority of biomaterials in use are designed such that they are void of specific ligands for MDM receptors, and therefore do not mark the material for phagocytosis. However, due to the protein coat on biomaterials following implantation, MDMs may still interact with biomaterials through this protein layer. The inflammatory polarization of MDMs oc-

curs as a result of simultaneous exposure of INF-γ and tumor necrosis factor (TNF)[81]. Ligation of these receptors results in intracellular signaling pathways that lead to cytokine secretion, enzyme release and/or phagocytosis. This MDM polarization is alternatively known as classically activated or M1 macrophages.

1.4.3 Anti-Inflammatory (M2) Polarization

As the damage to the wound site is reduced, MDMs begin the process of repair and regeneration. MDMs are capable of the recruitment and direction of more synthetic cells, such as fibroblasts and endothelial cells, leading to angiogenesis and repopulation[83]. In addition, MDMs support wound healing by remodeling extracellular matrix proteins by phagocytosis and degradation[69]. These MDMs typically fall within the category of alternatively-activated or M2 macrophages[81].

In general, a balance between these two macrophage polarizations is required to ensure that a biomaterial implant is biocompatible. As an example, MDMs produce and secrete a variety of enzymes including MMPs, acid hydrolases, and serine proteases, which have not been incorporated into the macrophage polarization spectrum. These enzymes play important roles in the inflammatory and wound healing process and therefore should not be overlooked especially when it comes to cellular interactions with collagenous biomaterials. A further understanding is required to fully characterize the macrophage response in terms of enzyme secretion and their biological performance with collagenous scaffolds. *In vitro* studies, such as those de-

scribed in this thesis, are one pathway towards obtaining such understanding of a material's biological performance.

1.5 Sources of Macrophages for *in vitro* Experimentation

In vitro studies have typically utilized human macrophages derived from two sources: (i) primary cells from humans or (ii) immortalized cells from a cell line. Each of these sources has characteristic advantages and disadvantages. The primary advantage of an immortalized cell line stems from the ease of culture and the homogeneity of the cells[84]. Cell lines show little variation between cultures and are more robust than primary cells. Specifically, monocyte-like cell lines are readily available and do not require human donors, research ethics clearance or timely isolation procedures, saving time and research costs. A variety of monocytic cell lines have been utilized as representative macrophages, although few are human-derived, and even fewer have been used to study biomaterial-cell interactions.

One study comparing cell lines has found that U937 cells are an ideal choice for studying biomaterial interactions[85]. Furthermore, due to the numerous comparisons made with U937s and monocyte derived macrophages, more confidence exists in using these cells as replacements for human cells. The U937 cell line was derived from the pleural effusion of a patient with diffuse histiocytic lymphoma[86]. It is an established pro-monocytic cell line that can be chemically differentiated, using phorbol myristate acetate to assume a macrophage phenotype[87]. This differentiated cell

type produces and releases both collagenase and collagenase inhibitors, which makes it a relevant choice for studying reactions to natural biomaterials[84].

The primary disadvantage of a cell-line is that it does not represent a physiologically normal, typical macrophage, and therefore cell line results may not be clinically relevant[88]. Despite the heterogeneity and the variation between human donors, as well as the lengthy culturing protocols, primary cells derived from humans remain the preferred cell source to use in studying biomaterial interactions.

In general, the interactions of macrophages with collagenous materials, especially tissues that have been crosslinked for use as heart valve replacements have been poorly examined. A greater understanding of the initial and long-term interactions of macrophages with these crosslinked matrices is essential to adequately predicting and enhancing the performance of these new heart valve matrices.

Recent work by Ariganello *et al.*[39,89,90] has investigated the differentiation method of U937s and MDMs on decellularized bovine pericardium and polystyrene. It compared two separate differentiation models: (i) a direct differentiation of primary monocytes on the individual surfaces in question and (ii) an indirect method in which cells were cultured on the same surface initially, followed by trypsinized activation prior to exposing the cells to the different substrates. Comparisons of the enzymes released between the trypsinized activation model of mature MDM and the directly differentiated monocytes correlate with studies that have shown trypsinization to be an activating process[91]. In that study, the biomaterial surfaces were investigated for their ability to *directly* induce the differentiation of pro-monocytic U937s, without the addition of exogenous growth factors or cytokines. In this way, impor-

tance was placed on how the material surface stimulated the release and/or expression of cytokines and enzymes, without confounding variables and/or 'priming' the U937s toward a specific macrophage differentiation pathway.

Using the knowledge gained from the work by Ariganello *et al*.[39,89,90] as a background, the present thesis attempts to investigate the method of direct differentiation of U937s on decellularized bovine pericardial matrix that has been crosslinked with two common crosslinkers, observing the response of the macrophage-like cells to the surfaces.

Chapter 2: Hypotheses and Rationale

2.1 Rationale

This project was developed to further the knowledge of macrophage interactions with tissue-derived crosslinked biomaterials. The successful use of animal heart valves/tissues in replacing damaged counterparts in humans depends on the ability to adequately preserve such tissues. Through the use of glutaraldehyde, crosslinks are added to the collagenous tissues to increase resistance to enzymatic degradation, and to increase the long-term durability. However, cytotoxicity and calcification issues have been associated with this industrial standard of crosslinking biomaterials. The crosslinker, EDC has been proposed as the alternative crosslinking agent to glutaraldehyde[92].

The objective of this thesis is to establish the macrophage cellular response on decellularized bovine pericardium that has been fixed with two well-examined crosslinking agents. Bovine pericardium represents a common biomaterial that is being used as a decellularized matrix in tissue engineering and more particularly, as a bioprosthetic heart valve material. Specifically, the tissue will be fixed using either glutaraldehyde, or the alternative crosslinking agent, EDC. The specific cells chosen for this study are the macrophage-like cells, derived from the immortalized cell line, U937. The cells will be seeded onto the fixed pericardial surfaces, as well as onto untreated decellularized pericardium. The cellular response will be characterized through DNA analysis, viability assays, cytokine analysis by ELISA, and cellular morphology using scanning electron microscopy.

Bovine pericardium was chosen as the decellularized matrix material to investigate for both scientific and practical reasons. Chemically treated bovine pericardium has a long history of use as a biomaterial in the body, and particularly in the cardiovascular system, where it successfully withstands dynamic mechanical loading and blood interaction[93,94]. Crosslinking pericardium that has been decellularized provides a simplified *in vitro* model for a heart valve matrix that is void of cells and cellular debris. Additionally, it has been used for more than 30 years in bioprosthetic valves, and it is a practical choice for the production of a decellularized valve or patch material[95]. The use of pericardium is sensible from the point of view of creating diverse valve sizes to treat young and old patients, and from an experimental perspective, pericardium provides a large source of tissue from a given animal compared to the small amount of tissue available from valve leaflets.

2.2 Hypotheses

The research done for this thesis can be separated into three smaller studies, each generating its own hypothesis. The first study uses scanning electron microscopy to observe U937 macrophage-like cells on the various surfaces. The second study measures cellular attachment and membrane integrity of U937 macrophage-like cells on the various surfaces. The third study measures released cytokines and matrix metalloproteinases from adherent U937 macrophage-like cells on the four surfaces.

HYPOTHESIS 1:

U937 macrophage-like cells seeded onto the glutaraldehyde-treated pericardial matrix will be morphologically different than cells seeded onto the carbodiimide-treated and control matrices.

HYPOTHESIS 2:

The quantity of U937 macrophage-like cells adherent on the glutaraldehyde-treated pericardial matrix will be significantly less compared to the carbodiimide-treated or control matrices.

HYPOTHESIS 3:

U937 macrophage-like cells on the untreated decellularized bovine pericardium will release less pro-inflammatory proteins, as compared to the cells on the two crosslinked matrices.

Chapter 3: Materials and Methods

All of the studies presented in this thesis employ common testing methodologies and statistical analysis as described in this chapter. Figure 3-1 illustrates the experimental approach used for this research. Bovine pericardial samples were decellularized and divided into two groups based on treatment: (1) decellularized pericardial matrix treated with glutaraldehyde or carbodiimide, and (2) untreated decellularized pericardial matrix. An untreated control surface, tissue culture polystyrene was also used throughout this research. Pro-monocytic U937 cells were then seeded onto each of the four surfaces and allowed to differentiate for 72 h with the addition of PMA. Following differentiation, cellular attachment was measured through analyzing the DNA of the U937 macrophage-like cells. Their morphology was observed using SEM, and the concentrations of their cytokines and enzymes measured using activity determination assays and enzyme-linked immunosorbent assay (ELISA).

3.1 Preparation of the Surfaces

Unless otherwise specified, all reagents were purchased from Sigma-Aldrich Inc. (Oakville, ON Canada). Where applicable, volume/volume percentages were used instead of molar concentrations.

3.1.1 Polymer Surfaces

Tissue culture polystyrene (TCPS) 48-well plates were used for TCPS surfaces, whereas sterile TCPS discs (Starstedt, Newton, NC, Cat. No. 83.1840.002) were

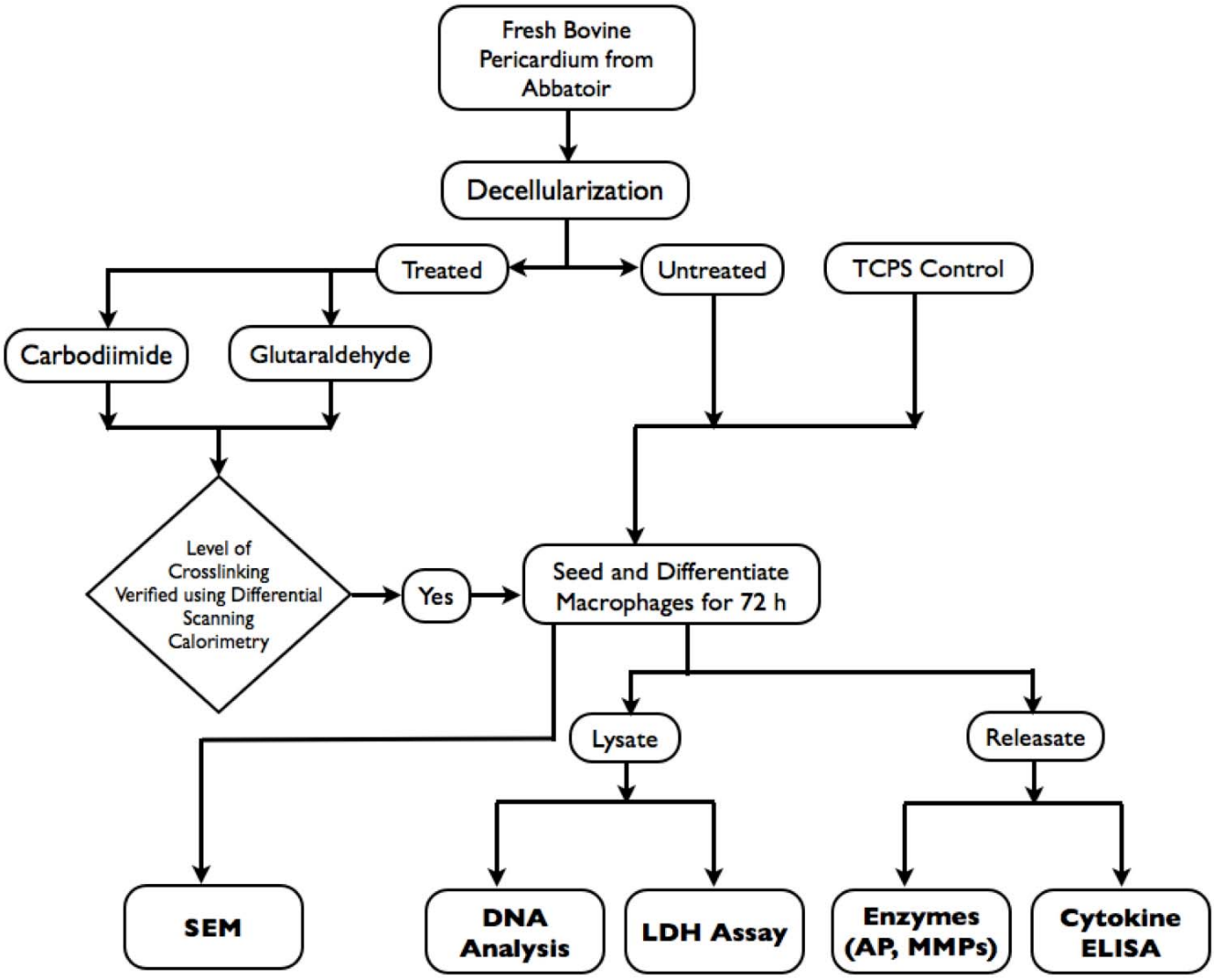

Figure 3-1: Outline of experimental methodology.

Each square of decellularized pericardial matrix follows a path from the top of the figure to the bottom and is included in one or more experiments at each level.

required for microscopy experiments. BD Falcon™ Plates (Cat. No. 353047) were used exclusively for cell culture as previously described by Ariganello *et al*.[39,89].

3.1.2 Pericardial Harvest and Decellularization

Fresh hearts were collected from 24-30 month old steers at a local abattoir (OH Armstrong Ltd., Kingston, Nova Scotia) and the pericardium cleaned of fat to allow for access to the tissue. Hearts were oriented for dissection with the ventral side facing upwards as determined by the rightward curvature of the aorta. The base-to-apex axis was defined as a line that would connect the point where the aorta met the heart to the apex of the heart. Beginning 1-2 inches down from the aorta, a ~10 cm cut was made perpendicular to and centered around, this base-to-apex axis. Continuing from this initial cut, a 10 cm^2 piece of pericardium was excised from the heart. A triangular notch placed in the upper left- hand corner was used for orienting the tissue for further dissection. During dissection, pericardial tissue was kept moist by applying phosphate buffered saline (0.1 M, pH 7.4) (PBS) with a pasteur pipette. The pericardial tissue was then transported back to the laboratory in PBS on ice. Prior to the decellularization procedure, the pericardial tissue was dissected and transferred to a cutting board and oriented in the base to apex direction once more. The pericardium was processed within 5 hours of collection. The 10 cm x 10 cm piece from the anterior side of the pericardium, was cut into four 35 mm x 35 mm samples that were individually decellularized.

The decellularization process was a modification of the protocol used by Courtman et al.[36]. The solutions used are described in detail in Table 3-1. All solutions, with the exception of PBS and Solution A, were made fresh within 12 hours of use,

Table 3-1: Aqueous Solutions used in Decellularization Protocol.

Solution A	Solution B	Solution C	Enzyme Cocktail
10 mM Tris Base 5 mM EDTA 0.5% antibiotic solution (contains 10,000 U/mL penicillin, 10,000 mg/mL streptomycin) 0.35 mL/L PMSF solution (5g PMSF in 100 mL of 100% ethanol) pH 8.0	50 mM Tris Base 1.5 M KCl 5 mM EDTA 1% Triton X-100 0.5% antibiotic 0.35 mL/L PMSF pH 8.0	50 mM Tris Base 1% Triton X-100 pH 9.0	2,500 U/mL DNAse[1] Hanks' Solution 2 mg/mL RNAse[2] Hanks' Solution

EDTA: ethylene diamine tetraacetic acid; PMSF: phenylmethylsulfonyl fluoride;

[1]DNAse 1, Type II from bovine pancreas, [2]RNAse A, Type III A from bovine pancreas

and the process proceeded under continuous mixing. The decellularization treatment began with three, 30 min incubations in room temperature PBS containing 1% penicillin/streptomycin and amphotericin B solution. Samples were then washed in Solution A for ~ 36 h at 4°C, with fresh solution exchanged every 12 h. Immediately thereafter, the samples were placed in Solution B for 24 h at 4°C, with fresh solution replaced after 12 h. Samples were then washed at room temperature with distilled water for 30 min, and rinsed in Hanks' solution prior to incubation for 60 min at 37°C in the enzyme cocktail.

Following the enzyme digest, all exchanges were performed in a laminar flow hood under sterile conditions. The samples were rinsed again with Hanks' solution, and washed with Solution C at room temperature for 24 h, with new solution replaced after 12 h. The samples were rinsed in PBS containing 1% antibiotic/antimycotic solution for 30 min, then in PBS containing only 1% antibiotic solution twice for 30 min prior to a 48 h wash in PBS containing 1% antibiotic solution at room temperature. Samples were finally stored at 4°C in sterile bottles filled with PBS containing 1% antibiotic solution until needed, but not longer than 4 months. The antimycotic, amphotericin B, was required to minimize fungal contamination of the pericardium. Prior to placing the tissue into culture wells and seeding with cells, an additional 1 h rinse in PBS containing antibiotic (1%) and antimycotic (10%) was found to greatly decrease fungal contamination during the 48 h incubation period. Two 30 min PBS rinses as well as an overnight incubation in PBS were used to rinse residual antimycotic from the tissue prior to cell seeding. Antimycotic was not included in the cell media during the culture periods because it interfered with the

spectrophotometric assays and its absorption could alter the response of the cells to the surfaces[96].

3.1.3 Crosslinking Pericardium with Glutaraldehyde

A square 35 mm by 35 mm piece of pericardium was immersed in 350 mL of the glutaraldehyde-crosslinking solution for 1 hour. The glutaraldehyde-crosslinking solution was made up of glutaraldehyde from a 50% electron microscopy grade glutaraldehyde stock solution in 0.1 M phosphate buffer to a final concentration of 0.5% (pH 7.4). The phosphate buffer solution was prepared by combining 0.1 M NaH_2PO_4 with 0.1 M Na_2HPO_4 (BDH, Toronto, ON) until a pH of 7.4 was reached. After fixation, the tissue was removed from the crosslinking solution and rinsed in three sets of 30-minute washes. The first 30-minute wash was in PBS (three washes at 10 minutes each). This was followed by a 30-minute wash in a 0.1 M glycine solution buffered in 0.1 M phosphate buffer (pH 7.4) to inactivate the unreacted or partially reacted glutaraldehyde (three washes at 10 minutes each)[53]. The tissue was finally washed for 30 minutes in a PBS solution (three washes at 10 minutes each). The crosslinked tissue was stored at 4ºC for 24 h before being used in cell culture.

3.1.4 Crosslinking Pericardium with 1-ethyl-3-(3-dimethylaminopropyl)-carbodiimide

The EDC-crosslinking protocol was completed according to the methods described by Lee *et al*.[54] A 1.15% by weight 1-ethyl-3-(3-dimethylaminopropyl)-carbodiimide hydrochloride (EDC) solution with a 2:1 molar ratio of EDC to

N-hydroxysuccinimide (NHS) was prepared by dissolving 1.15 g of EDC and 0.35 g of NHS in 100 mL of distilled water. The EDC solution's pH was then adjusted to 5.5 by the addition of 1 M HCl or 1 M NaOH. The 35 by 35 mm square of tissue was immersed in the EDC solution within an hour of solution make-up. The pH was monitored using a pH meter (Cole-Palmer, Chicago, Il) and a pH of 5.5 was maintained during crosslinking[97]. After 24 h, the tissue was removed from the crosslinking solution and washed in 0.1 M Na_2HPO_4 for 30 minutes (three washes at 10 minutes each) to hydrolyze any remaining NHS-activated carboxylic acid groups[54]. Subsequently, the tissue was washed for 30 minutes with a phosphate buffered saline solution (three washes at 10 minutes each). The crosslinked tissue was stored at 4°C for 24 h before being used in cell culture.

3.1.5 Crosslink Verification using Differential Scanning Calorimetry

To validate the effectiveness of the fixation process with either glutaraldehyde or carbodiimide, differential scanning calorimetry (DSC) was used. Bovine pericardium has a denaturation temperature ranging from 68 to 85°C for untreated tissue and glutaraldehyde/carbodiimide crosslinked tissue, respectively[54]. Calorimetry was performed using a TA Instruments Q-200 DSC (TA Instruments Inc., New Castle, Delaware, USA) calibrated with Indium and Tzero™ Sapphire standards. Tissue samples were blotted dry and hermetically sealed into 20 μL aluminum DSC pans, ensuring that each pan was completely filled with tissue in good contact with the pan. Each sample-containing pan was tested against an empty identical reference

pan at a programmed temperature range of 2°C per minute starting at 20°C and finishing at 85°C for untreated samples. For glutaraldehyde and carbodiimide-treated samples, the finishing temperature was 100°C. At the completion of each run, the denaturation endotherm onset temperature, T_{onset}, T_{peak}, and area under the endotherm peak were calculated using DSC Advantage Q series software version 2.3.0.251. This information along with all raw data files, were saved digitally. The onset and peak temperatures were compared to known values in the literature and the crosslinking process was deemed effective if the values were close to the published temperatures and repeatable from run to run.

3.2 Preparation of Cell Culture Wells

Decellularized bovine pericardium (DBP) was cut into 10 mm diameter discs and placed into individual wells of a 48-well plate. The fibrous layer of the matrix was facing down so that cells would be seeded on what would have been the mesothelial (heart-facing) surface prior to decellularization. During the biochemical studies, an experiment was defined as differentiating the macrophage-like cells for 72 h, lysing the cells to measure their DNA to determine their adherence to the surface, and collecting the releasate and lysate from each of the surfaces for further analysis of cytokines, enzymes, and scanning electron microscopy (SEM). Each experiment consisted of 6 discs of DBP, glutaraldehyde-treated DBP, carbodiimide-treated DBP, and tissue culture polystyrene, with 3 of the discs from each substrate serving as unseeded controls. All surfaces were incubated in PBS containing 1% antibiotic solution overnight at 37°C and 5% CO_2 to equilibrate the surfaces prior to cell seeding.

3.2.1 U937 Cell Culture

The immortalized cell line U937 was obtained from the American Type Culture Collection (ATCC; No. CRL-1593.2) and maintained as a pro-monocytic cell suspension at 37°C, under conditions of 5% CO_2 and 100% humidity, and fed every other day with RPMI-1640 supplemented with 1 mM sodium pyruvate, penicillin (100 U/mL), streptomycin (100 mg/mL), and 10% fetal bovine serum as previously described in detail[98]. Only cells that were between passages 8 and 18 were used for differentiation into macrophage-like cells (as recommended by the supplier, ATCC). Aliquots of cells were frozen prior to passage 18 and stored at -80°C for future use. The cells were differentiated by directly seeding onto each of the four surfaces (DBP, glutaraldehyde-treated DBP, carbodiimide-treated DBP, and the control TCPS) 800,000 cells/well (concentration of 2 million cells/mL) in the presence of 100 nM PMA for 72 hours as described previously by Ariganello *et al*. [90]. The PMA was used to maintain their fully differentiated, adherent state[98].

3.2.2 DNA Determination

Cells were lysed after 72 h incubation and immediately analyzed for DNA following the protocol by Matheson *et al*.[98]. Briefly, Hoechst dye no. 33258 (Fisher Scientific) (0.1% mg/mL) was diluted with Tris buffer (0.01 M Tris, 0.001 M EDTA, 0.2 M NaCl), pH 7.4) on the day of analysis. Cell lysate (15 µL) was added to the dye (100 µL) into a 96-well plate (Microfluor 2 Black; VWR, Mississauga, Canada) and read against a DNA standard (10 – 300 ng DNA) (prepared with the same amount of Tri-

ton X-100 which was in the lysate sample) in a fluorescence microplate reader. All the data for enzyme and cytokine release from U937 macrophage-like cells were normalized to the number of live, adherent cells.

3.2.3 Acid Phosphatase Activity Determination

Cell lysate and releasate were assayed for acid phosphatase activity after 72 h of incubation of cells on all four surfaces. Acid phosphatase activity was measured by the production of p-nitrophenol via the hydrolysis of p-nitrophenylphosphate, as described previously[91]. The technique was a modification of that of Akisaka *et al*.[99]. Briefly, aliquots of lysate (25 μL) and releasate (150 μL) were added to p-nitrophenylphosphate disodium solution (10.8 mM) and citrate buffer (64 mM sodium citrate, 10 mM NaCl, pH 4.8) and incubated for 30 minutes at 37°C. The reaction was stopped by the addition of 1.3 mL NaOH (0.1 M) and the absorbance read at 410 nm. Acid phosphatase activity was reported in units (a unit is defined as the release of 1 nmol of p-nitrophenol [ε= 16, 300 $cm^{-1}M^{-1}$] per minute at 37°C) and each activity value was normalized to the number of live, adherent cells determined by DNA analysis.

3.2.4 Scanning Electron Microscopy

To investigate cellular morphology and cell surface roughness after 72 h of culture, wells were fixed with 2.5% glutaraldehyde in PBS for 2 hours and rinsed in PBS. Samples were then dehydrated in aqueous ethanol, critical-point-dried, and

sputter-coated with a mixture of gold and palladium. Samples were imaged using a Hitachi S-4700 scanning electron microscope (Institute of Research in Materials Laboratory, Dalhousie University) at an accelerating voltage of 7 kV and current of 10 μA.

3.2.5 Lactic Acid Dehydrogenase Activity Assay

To ensure that the attached cells were healthy, lactic acid dehydrogenase (LDH), a cytoplasmic enzyme, was measured in the conditioned media of the cells after 72 h. Elevated levels of LDH are associated with tissue and cellular membrane breakdown and can be used as a marker for myocardial infarction and certain forms of cancer[100]. This colorimetric assay is based on the LDH-catalyzed conversion of pyruvate to lactate in the presence of NADH as previously described by Erfle *et al*.[101]. Briefly, pyruvate was quantified by the reaction with 2,4-dinitrophenyl hydrazine (color reagent) which results in the formation of a hydrazone product that absorbs light in the range of 400-500nm. Prior to performing the assay, the lysate samples from the cells cultured on each of the four surfaces were diluted 20 times using distilled water. Next, 2 mL of sodium pyruvate (0.75 mM) was added to 2 mg of NADH. Aliquots of 100 μL of the NADH/sodium pyruvate solution were incubated for 3-5 minutes at 37°C. Following this, 50 μL of the releasate or lysate was added and incubated for a further 30 minutes. Next, 100 μL of the color reagent was added and allowed to develop for 20 minutes at room temperature. The reaction was halted by the addition of 0.4 M NaOH and the absorbance read at 450 nm. The activities of the LDH assay are reported in LDH units (an LDH unit is defined by [initial moles of

pyruvate - final moles of pyruvate] x dilution factor/30 minutes) and each activity value was normalized to the number of live, adherent cells determined by DNA analysis.

3.2.6 Cytokine Enzyme-Linked Immunosorbent Assay

The cytokines studied, the pro-inflammatory cytokines IL-6 and TNF-α, and anti-inflammatory cytokines IL-1Ra and IL-10, were assayed using the Human Cytokine ELISA Ready-SET-Go!® kits from eBioscience (San Diego CA) following the protocol provided by the manufacturer. Briefly, 100 μL of releasate samples were incubated with a biotinylated antibody in a 96-well tissue culture polystyrene plate for 2 h at room temperature with shaking. After washing, the wells were incubated with secondary (detection) antibodies for 1 h at room temperature then incubated for 30 min with avidin horseradish peroxidase. Sample concentrations (pg/mL) were determined from median fluorescence intensities at 450 nm and compared to a logarithmic standard curve for each cytokine. The amount of cytokines released was normalized to the number of live, adherent cells determined by DNA analysis.

3.2.7 Matrix Metalloproteinase Enzyme-Linked Immunosorbent Assay

The matrix metalloproteinases studied, MMP-1, 2, and 9, were assayed using the Human MMP ELISA kit for Cell Culture Supernatant from RayBiotech (Norcross GA) following the protocol provided by the manufacturer. Briefly, 100 μL of releasate samples were incubated with a biotinylated antibody in a 96-well tissue culture

polystyrene plate for 2 h at room temperature with shaking. After washing, the wells were incubated with secondary (detection) antibodies for 1 h at room temperature, then incubated for 30 min with strepavidin horseradish peroxidase. Sample concentrations (pg/mL) were determined from median fluorescence intensities at 450 nm and compared to a logarithmic standard curve for each enzyme. The amount of matrix metalloproteinase released was normalized to the number of live, adherent cells determined by DNA analysis.

3.2.8 Statistical Analysis

All statistical analyses were conducted using JMP 5.01 software (SAS Institute, NC). Parametric data were analyzed using a 1-way analysis of variance (ANOVA) at an overall significance level of 0.05, and were Bonferroni-adjusted for multiple comparisons. Tukey's Honestly Significant Difference (HSD) *post hoc* was used to determine which means are significantly different from another and identify differences between the groups. Three separate experiments were performed, with three samples for each of the four substrates, therefore n=9 throughout. Data are presented as mean ± SD (SE), where SD = standard deviation and SE = standard error of the mean.

Chapter 4: Results

4.1 Outline

To reiterate, the purpose of this thesis was to study the macrophage response to decellularized bovine pericardium subjected to two modes of crosslinking (with glutaraldehyde or carbodiimide). The macrophage response on the crosslinked substrates was compared to untreated decellularized pericardium and tissue culture polystyrene as controls.

The first study investigated the morphology of U937 macrophage-like cells on these surfaces using scanning electron microscopy. Pericardial matrix was fixed with glutaraldehyde or carbodiimide and pro-monocytic cells were seeded directly onto the material surfaces. PMA was added to the growth media to differentiate the cells into macrophage-like cells. Differentiation took 72 h, as previously described by Matheson *et al*.[76] at 37°C and 5% CO_2 following which the cells were fixed with glutaraldehyde, dehydrated with ethanol, critical-point dried, and sputter-coated with gold and palladium. The prepared samples were imaged using a scanning electron microscope.

The second study investigated the quantity of the macrophage-like cells adherent to the substrates. This was done by measuring their DNA content. Following differentiation on the biomaterial surfaces, the media containing what the cells released (releasate) while in contact with the materials was collected. The macrophage-like cells were lysed and their DNA content was determined using the modification

by Matheson *et al*.[98] The fluorescence was measured at 460 nm using a microplate reader.

The third study investigated inflammatory proteins and matrix metalloproteinases released from U937 macrophage-like cells cultured on the four substrates. To determine if U937s released different amounts of these proteins on the four surfaces, releasates were analyzed for MMP-1, MMP-2, MMP-9, the pro-inflammatory cytokines IL-6 and TNF-α, and anti-inflammatory cytokines IL-1Ra and IL-10. These proteins were quantified using human ELISA kits. The amount of cytokines and matrix metalloproteinases released was normalized to the number of live, adherent cells via DNA analysis.

4.2 Verification of the Crosslinking Protocol Using DSC

Denaturation temperature studies were completed for each sample of crosslinked pericardial matrix tissue to evaluate the effectiveness of the crosslinking procedure. This was done using DSC and measuring the T_{onset} and T_{peak}. DSC measures the energetic changes during thermal transitions in collagen. In a typical set up, the DSC increases the temperatures of two pans at the same, constant rate of temperature change. One pan contains the sample of interest and the other is a reference pan. The difference in heat flow to the two pans is reported, giving a typical profile as shown in Figure 4-1 with apparent heat capacity on the vertical axis and temperature or time on the horizontal axis. These studies assessed the formation of exoge-

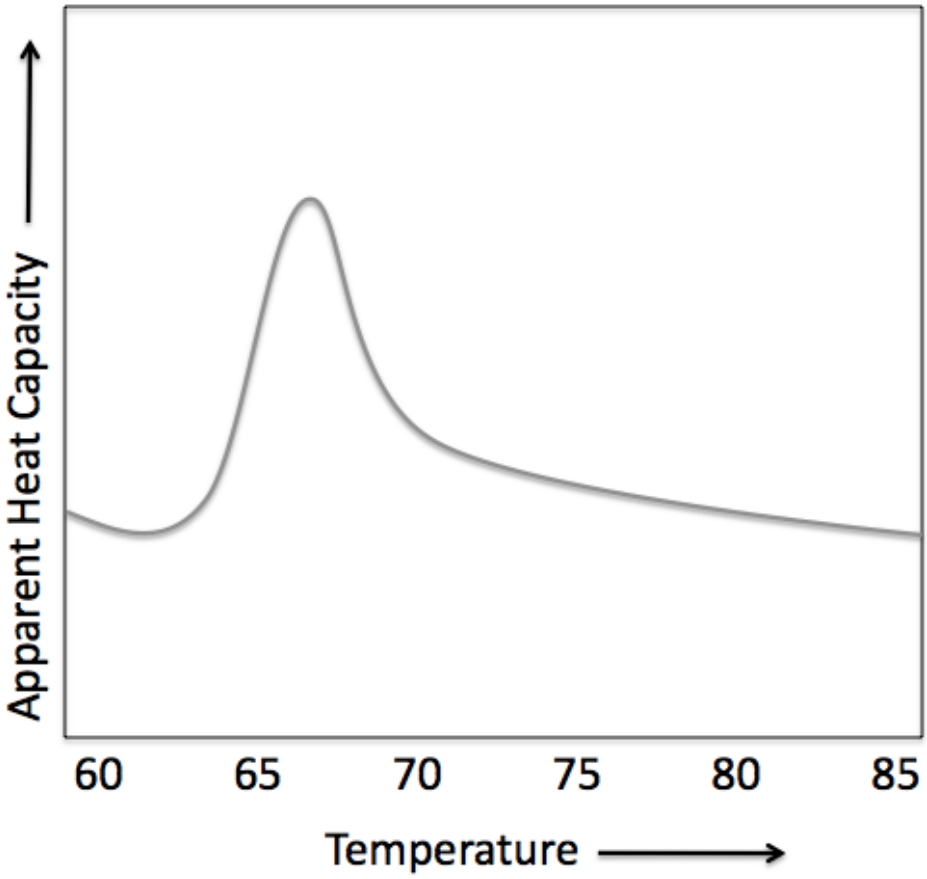

Figure 4-1: A representative DSC curve for collagen.
The positive peak indicates an endothermic process.

nous crosslinks in strips of decellularized bovine pericardial matrix treated with glutaraldehyde and carbodiimide. The resulting peak temperature was compared back to the untreated matrix. Glutaraldehyde and carbodiimide crosslinking both changed the denaturation temperature of bovine pericardium consistent with previous work done by Lee *et al*.[54] (Table 4-1). It has been demonstrated in previous glutaraldehyde studies that a plateau in the increasing denaturation temperature is reached within one hour using similar crosslinking conditions[53,54,97,102]; thus it was assumed that one hour was necessary for complete fixation. For crosslinking with carbodiimide, previous work found that the optimal fixation time was overnight at room temperature and an optimal pH of 5.5[54,97]. The results obtained from DSC, when compared to the values in the literature, verified the crosslinking protocols for glutaraldehyde and carbodiimide.

4.3 U937 Morphology using Scanning Electron Microscopy

The SEM micrographs of the U937 macrophage-like cells on the glutaraldehyde treated matrix surface are shown in Figure 4-2. At higher magnification, the cells appeared to have leaky membranes (when compared to the cells on the other surfaces). The size of the cells is consistent with that of a typical U937 cell (approximately 10 -20 μm)[103]. Furthermore, although this was not quantified, there appeared to be fewer cells on the glutaraldehyde-treated surfaces, and the cells appeared to be singular rather than being clustered or clumped as on the other surfaces. The

Table 4-1: Peak Temperatures Determined using DSC with Respective Literature Values.

Surfaces	Experimental Values	Literature Values[54,105]
Untreated Decellularized Pericardial Matrix	66.9 ± 1.3°C	65.7 ± 0.4°C
Glutaraldehyde-treated Decellularized Pericardial Matrix	83.7 ± 0.1°C	85.3 ± 0.4°C
Carbodiimide-treated Decellularized Pericardial Matrix	83.6 ± 0.2°C	86.0 ± 0.3°C

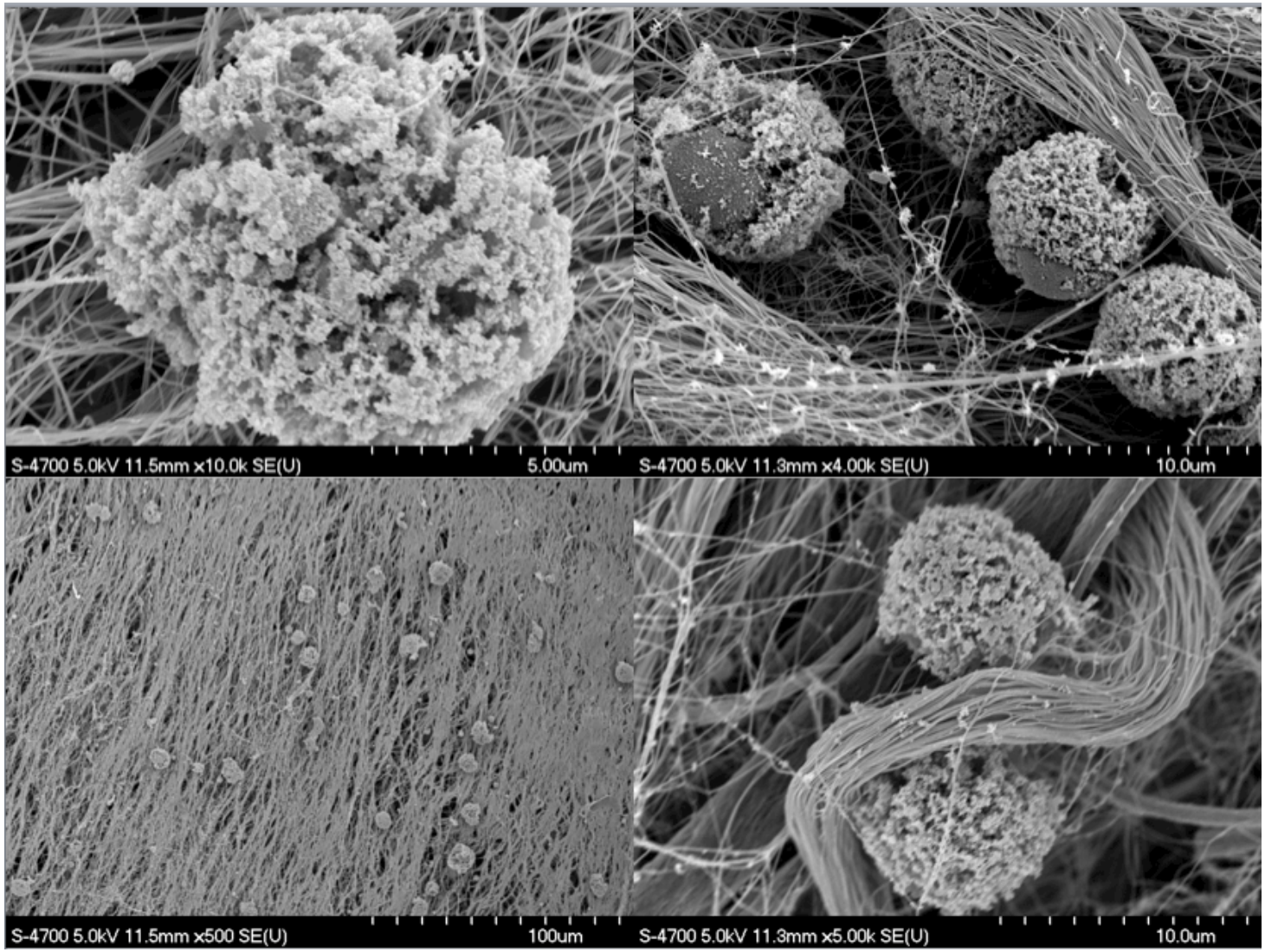

Figure 4-2: Scanning electron images of U937 cells on glutaraldehyde-treated pericardial matrix surfaces.

At low magnification, the cells appear to be singular and few in number. With increasing magnification, the degraded/destroyed cellular membranes are evident.

appearance of the macrophage-like cells seeded on the carbodiimide-treated surfaces was considerably different (Figure 4-3). The cells had a petal morphology and were clustered together. The micrographs of the U937 macrophage-like cells on the untreated decellularized bovine pericardium are shown in Figure 4-4. Similar to the cells on the carbodiimide-treated surfaces, the cells on the pericardium were grouped and appeared to be healthy morphologically when compared to those on the glutaraldehyde-treated surface. The cells had small blebs covering their surfaces, differing than those on the carbodiimide. Finally, looking at the cells on the tissue culture polystyrene, they tended to be singular and to have fine extensions (filopodia) projecting outwards from their centers (Figure 4-5). This appearance is consistent with previous work done by Ariganello *et al*.[89].

4.4 Cellular Response to the Biomaterial Surfaces

4.4.1 Quantification of DNA and Lactic Acid Dehydrogenase Activity

The results from the DNA determination assay are shown in Figure 4-6. Previous work by McBane *et al*.[104] has established that DNA content can be correlated with cell viability, as well as the number of adherent cells on the substrates.
A significant difference in DNA content was observed between glutaraldehyde-fixed and carbodiimide-fixed substrates. Additionally, the amount of DNA on the tissue culture polystyrene differed significantly from that and the crosslinked surfaces. This significant difference in DNA amount between the crosslinked substrates suggests that the glutaraldehyde may have inhibited U937 attachment to the pericardial matrix surface, perhaps due to residual, potentially toxic glutaraldehyde not being ade-

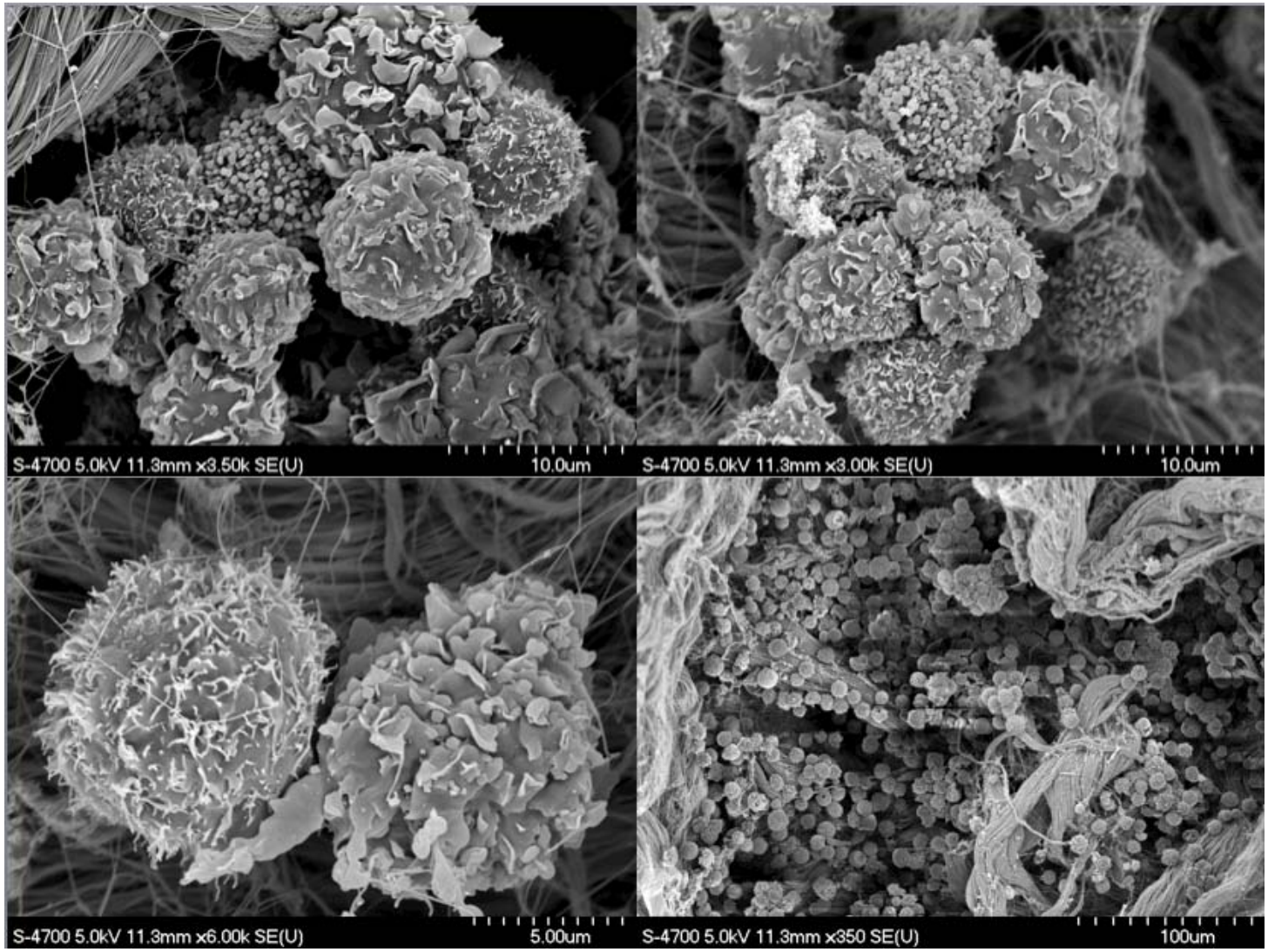

Figure 4-3: Scanning electron images of U937 cells on EDC treated pericardial matrix surfaces.

At low magnification, the clustering of the cells is evident. With increasing magnification, the observed petal morphology can be seen.

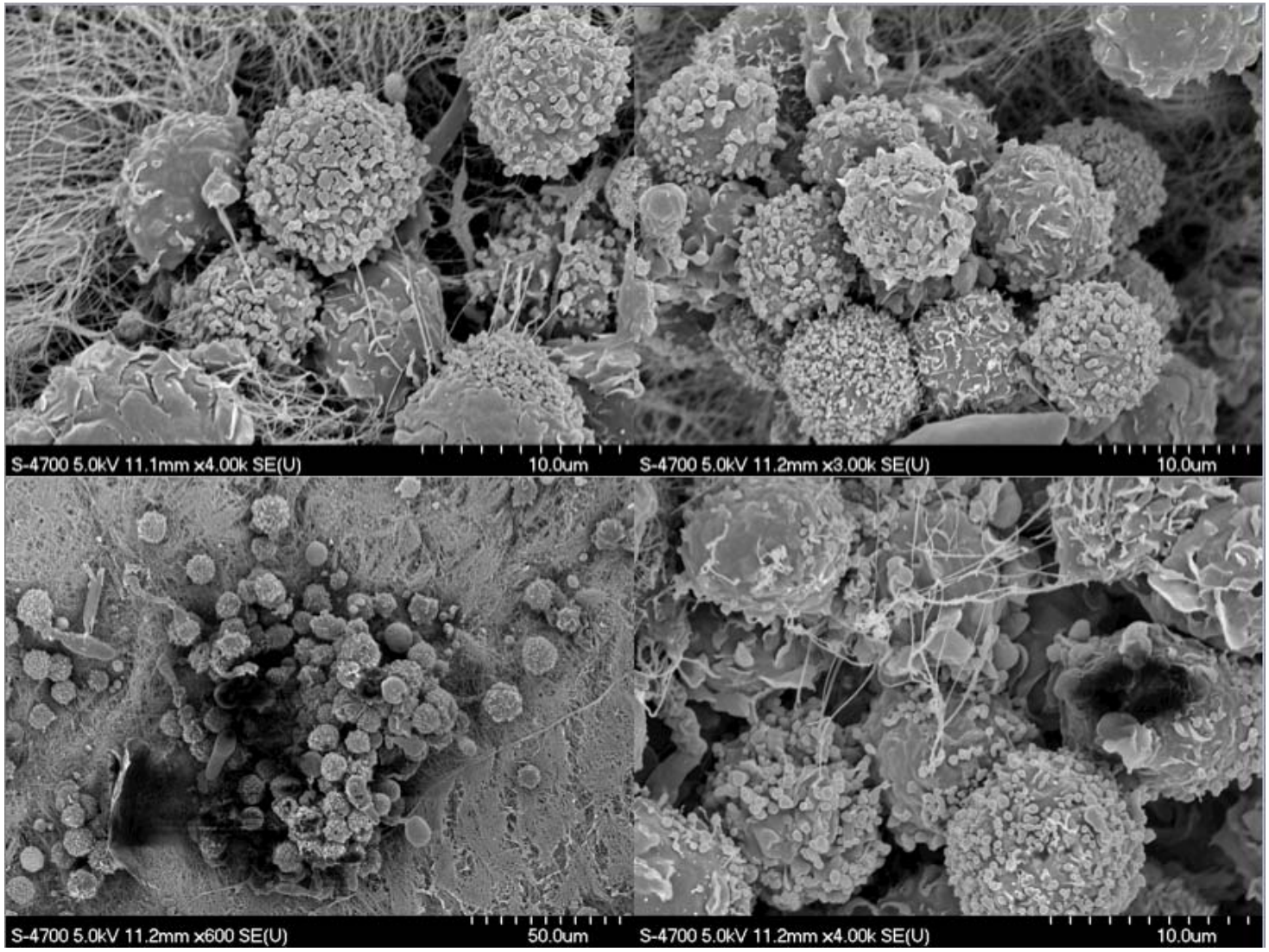

Figure 4-4: Scanning electron images of U937 cells on decellularized bovine pericardium.

At low magnification, the clustering of the cells is evident. With increasing magnification, a surface bleb morphology can be seen.

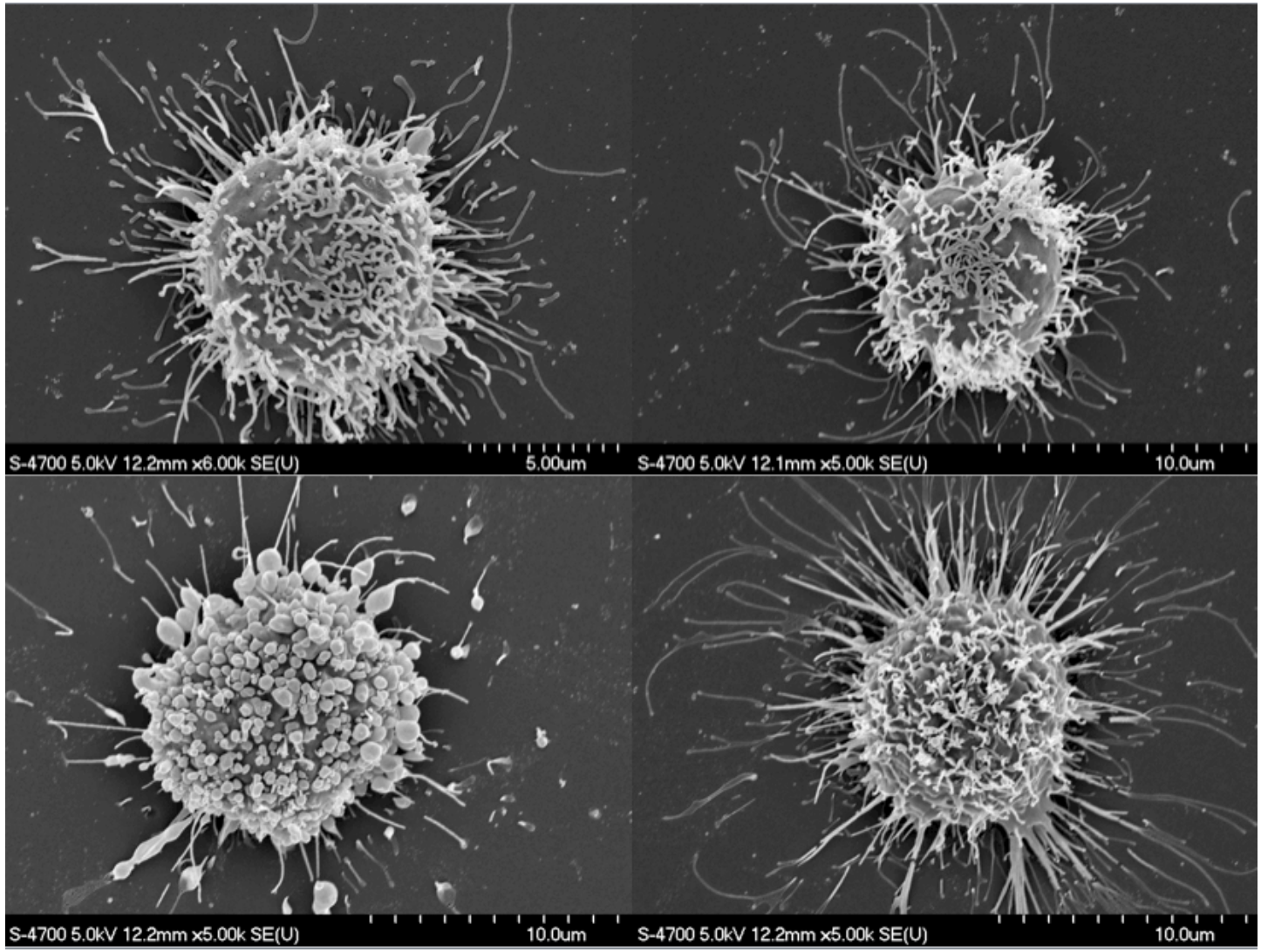

Figure 4-5: Scanning electron images of U937 cells on tissue culture polystyrene (TCPS)

Cells cultured on TCPS tend to spread and as a result, appear larger. Extending from each cell are fine filopodia, consistent with previous work done by Ariganello et al.[89].

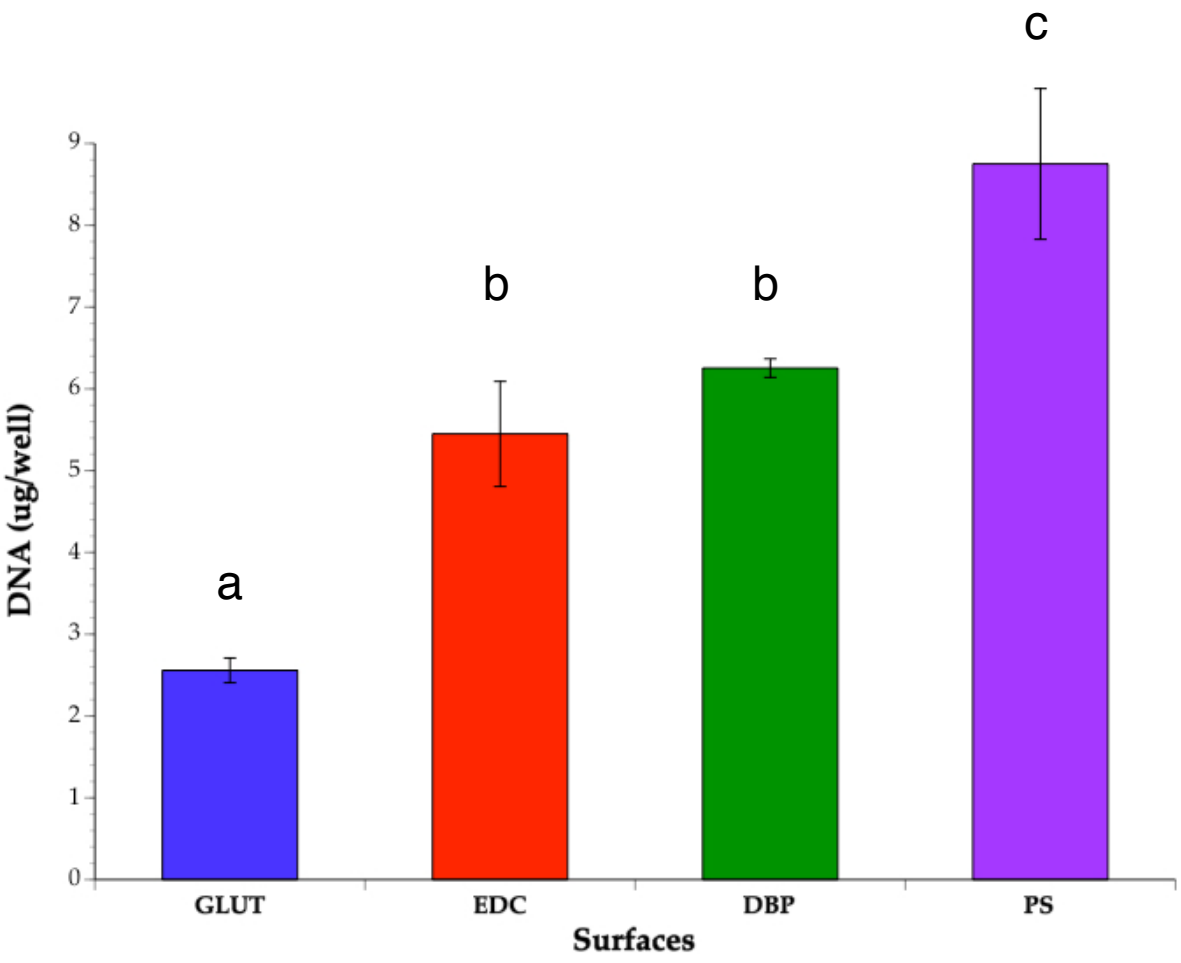

Figure 4-6: DNA Quantification

DNA values (μg per well) of the U937s cultured on each surface. Fewer cells were cultured on the glutaraldehyde-treated surface, compared to the other 3 surfaces. Different letters denote a significant difference from other surfaces at an overall significance level of P<0.008.

(Figure 4-7). There was a measurable amount of LDH activity in the releasate for the glutaraldehyde substrate, demonstrating that the cell membrane integrity was disturbed. Comparing the total LDH activity (releasate + lysate) from U937 cells on each of the surfaces, a significant difference was observed. Cells cultured on the glutaraldehyde-treated pericardium had significantly less total LDH activity than the other surfaces (Figure 4-8). It would be expected that the total LDH activity from the cells would be consistent across all surfaces, however; much of the activity from cells on the glutaraldehyde was lost, suggesting that the glutaraldehyde affected cell and membrane function.

4.4.2 Enzymatic Response to Biomaterial Surface

Cells cultured on glutaraldehyde and carbodiimide-treated surfaces contained lower amounts of acid phosphatase activity after 72 h compared to cells cultured on DBP and TCPS (Figure 4-9). Furthermore, cells on the glutaraldehyde-treated substrate differed significantly compared to those cells on the carbodiimide substrate in terms of their released acid phosphatase activity. Additionally, although there was no significant difference between the two crosslinked surfaces, cells exposed to both DBP and PS contained higher amounts of intracellular acid phosphatase activity (Figure 4-10). This is consistent with the similar increased cell attachment observed in cells cultured on DBP and TCPS.

Cells on all four surfaces released MMP-1, MMP-2 and MMP-9 (Figures 4-11, 12, and 13). Refer to Table 4-2 for the absolute values for the released MMPs. For every surface, U937s released significantly more MMP-1 activity compared to MMP-

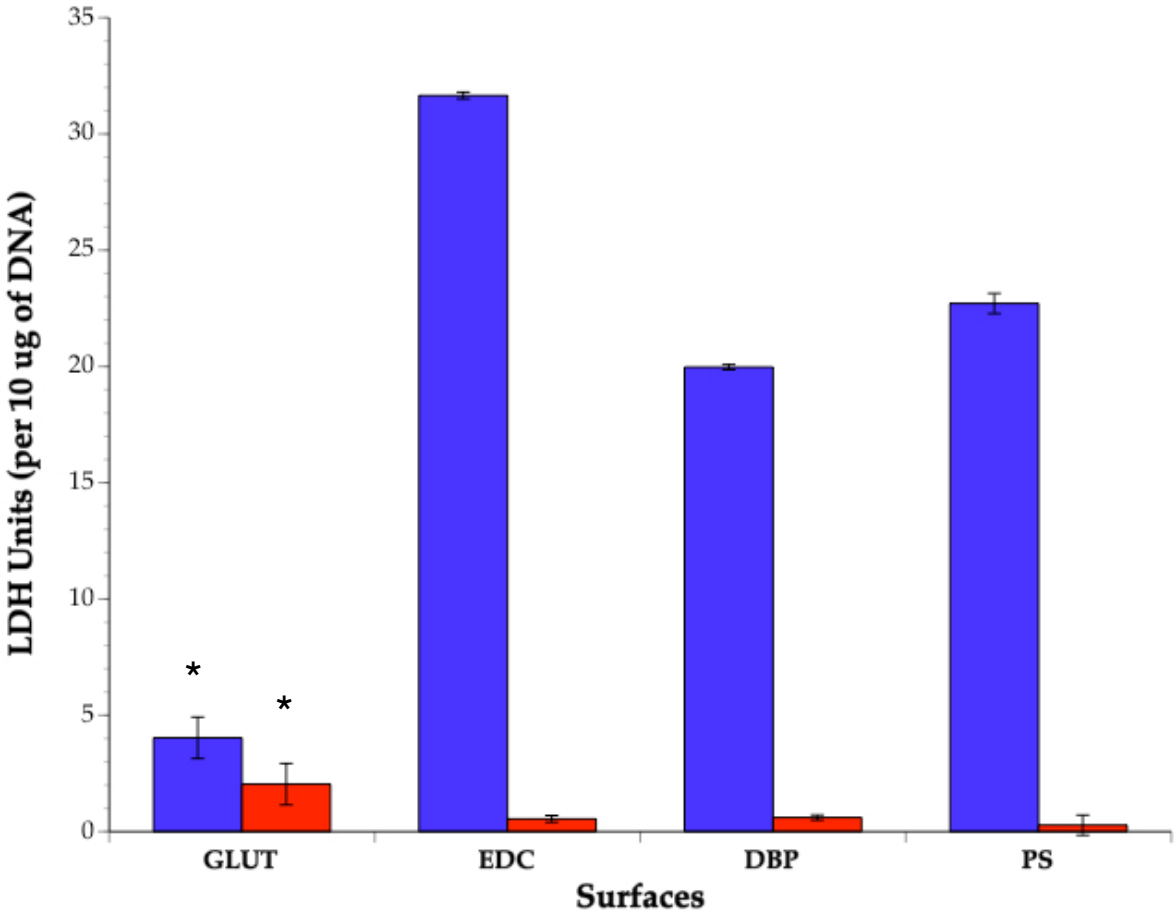

Figure 4-7: Lactic Acid Dehydrogenase Activity Assay

LDH units for U937 cells cultured on each surface normalized to 10 μg of DNA. Cell lysate (blue columns) and cell releasate (red columns) are reported. The intracellular LDH activity from cells on the glutaraldehyde-treated surface differed significantly compared to the other 3 surfaces. The released LDH activity from cells on the glutaraldehyde-treated surface differed significantly from the released activity on the other 3 surfaces (*)

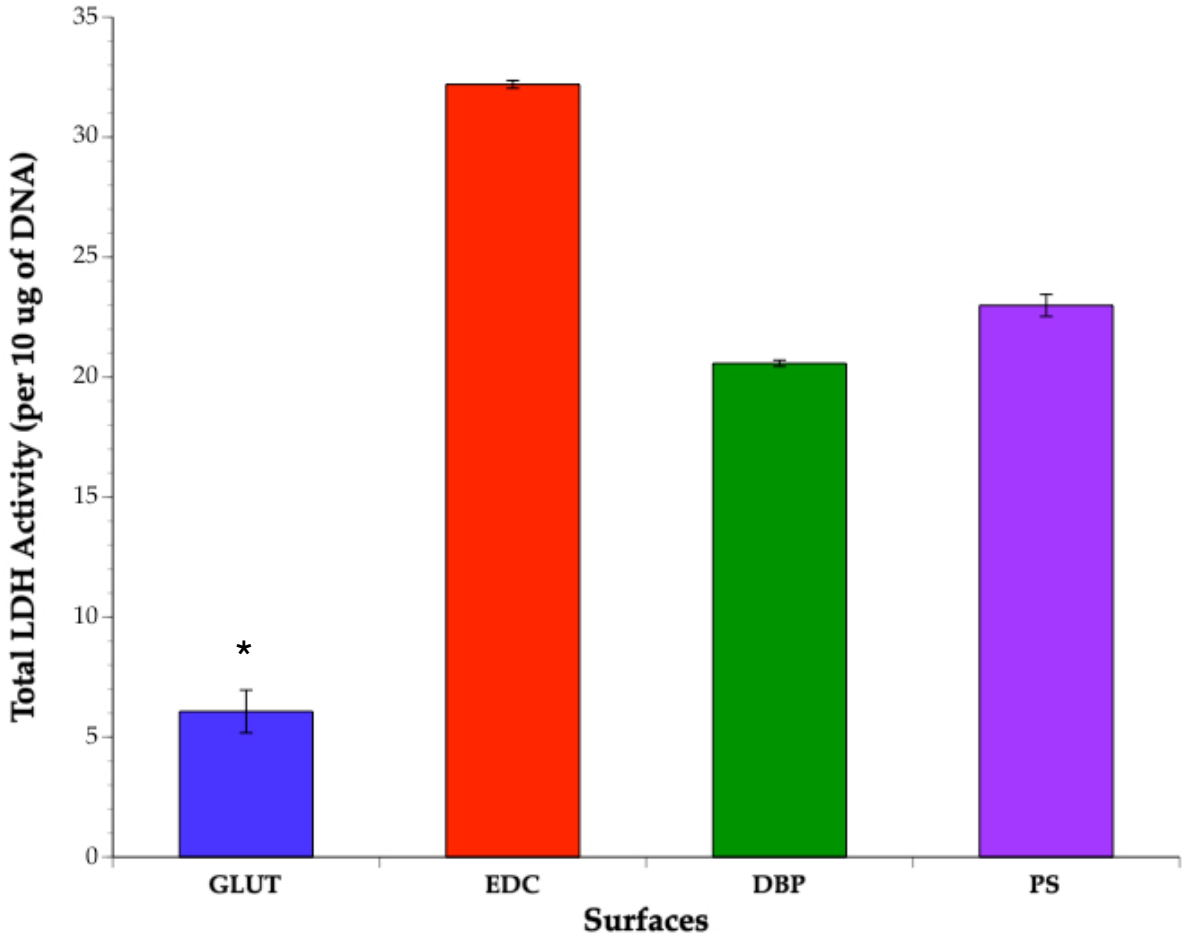

Figure 4-8: Total Lactic Acid Dehydrogenase Activity

LDH units for total LDH activity of U937 cells cultured on each surface normalized to 10 μg of DNA. The total LDH activity from cells cultured on the glutaraldehyde-treated surface differed significantly from the other 3 surfaces (*).

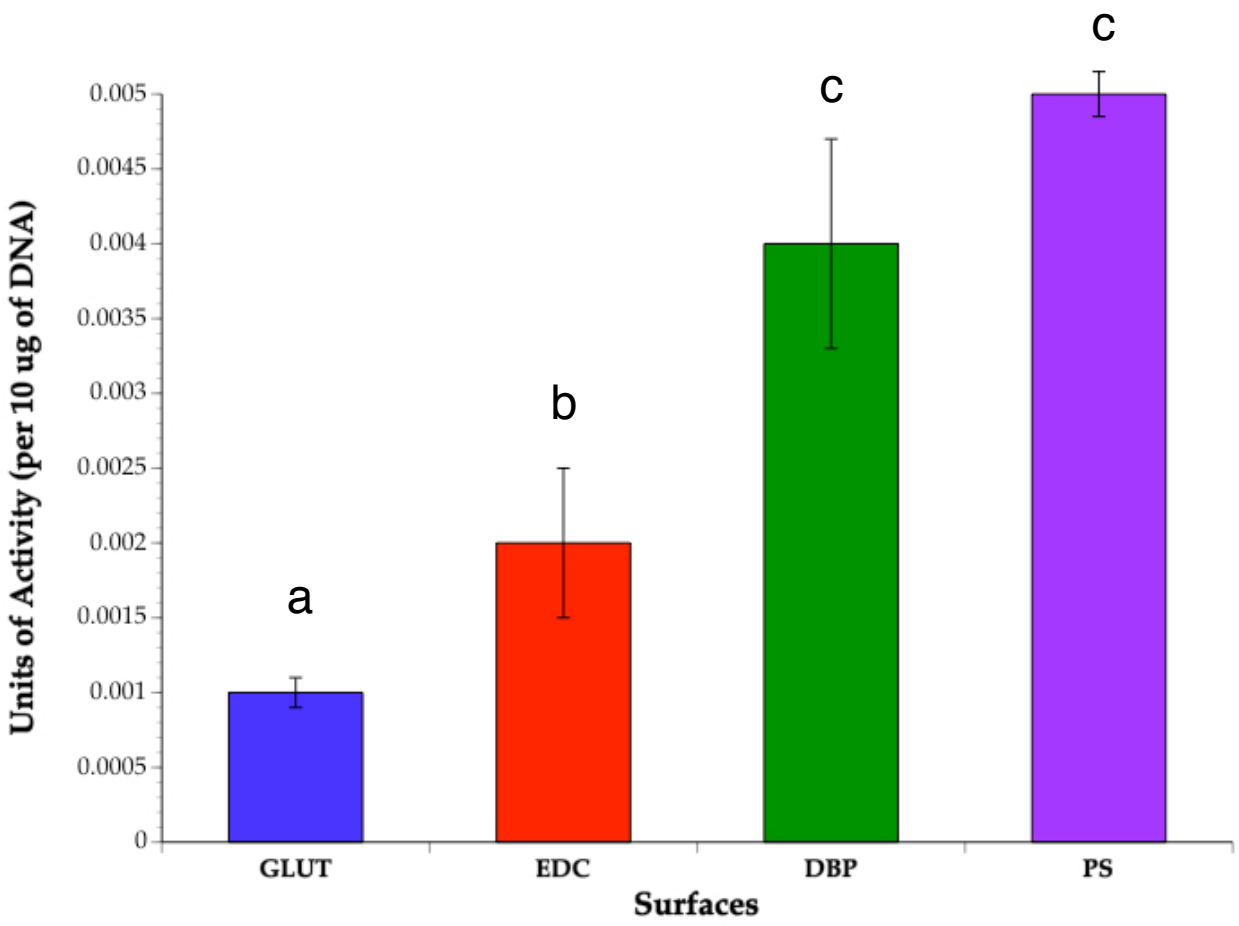

Figure 4-9: Intracellular Acid Phosphatase Activity from U937 Cells

Acid Phosphatase enzyme activity (units of activity/10 μg DNA) of cell lysate after 72 h cell culture on the four surfaces. Different letters denotes a significance difference from each other at an overall significant level of P<0.008

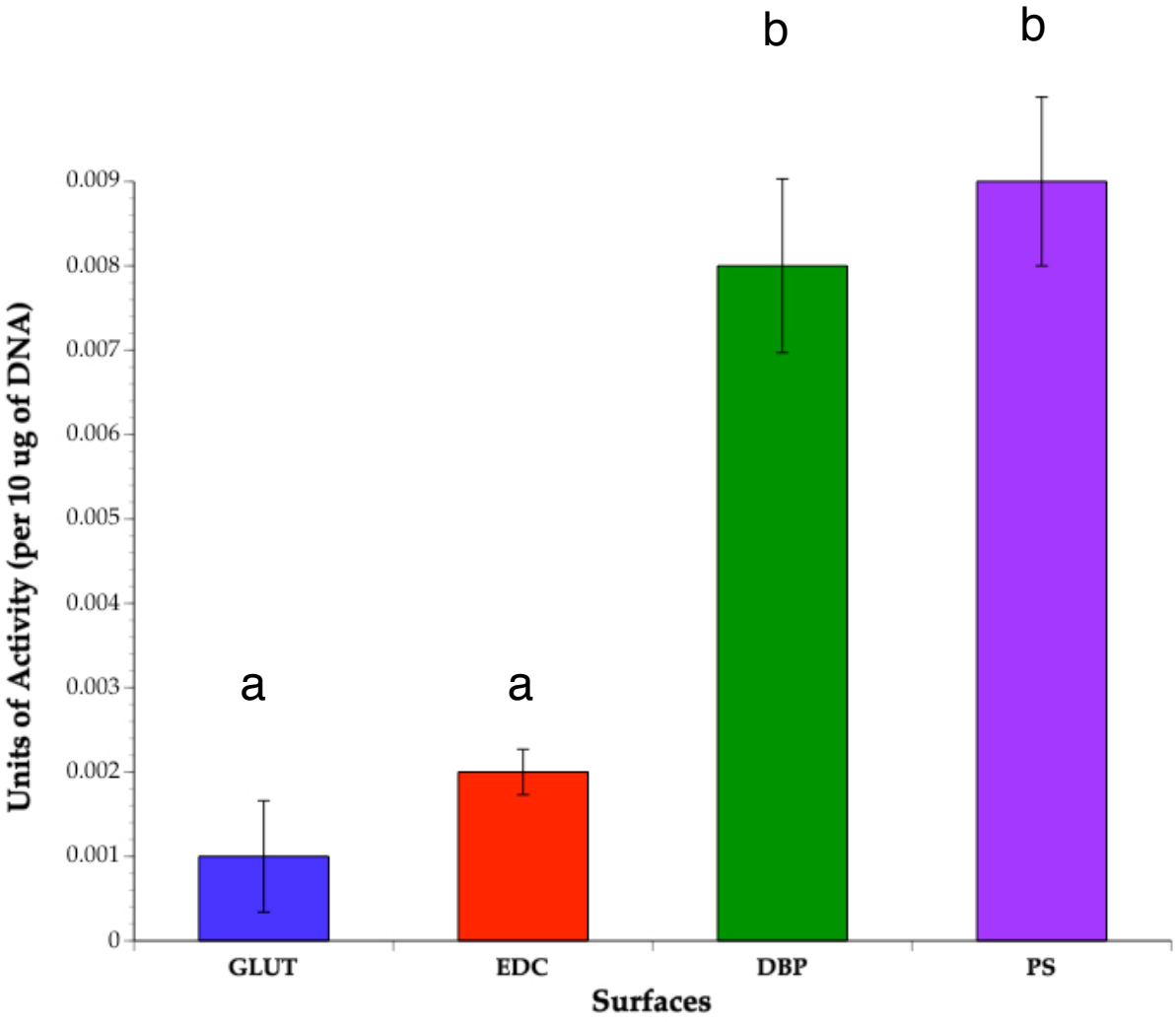

Figure 4-10: Released Acid Phosphatase Activity from U937 Cells

Acid Phosphatase enzyme activity (units of activity/10 μg DNA) of cell releasate after 72 h cell culture on the four surfaces. Different letters denotes a significance difference from each other at an overall significant level of P<0.008.

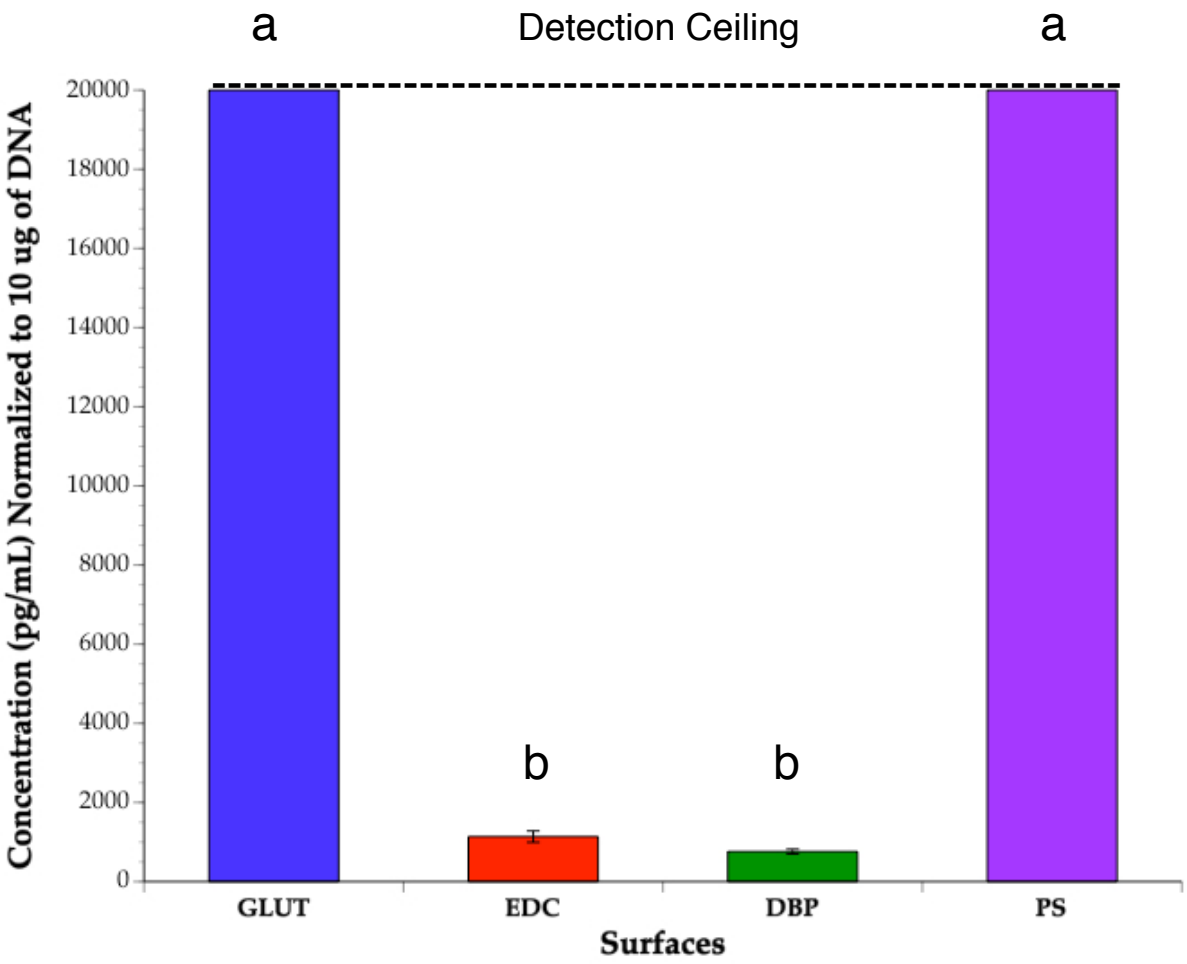

Figure 4-11: MMP-1 Released from U937 Cells

Matrix metalloproteinase 1 concentration as determined using an ELISA (pg/mL normalized to 10 μg DNA) of cell releasate after 72 h cell culture on the four surfaces. The concentrations of MMP-1 on the glutaraldehyde-treated and polystyrene surfaces were above the detection ceiling of the ELISA kit. Different letters denote a significant difference from other surfaces at an overall significance level of P<0.008.

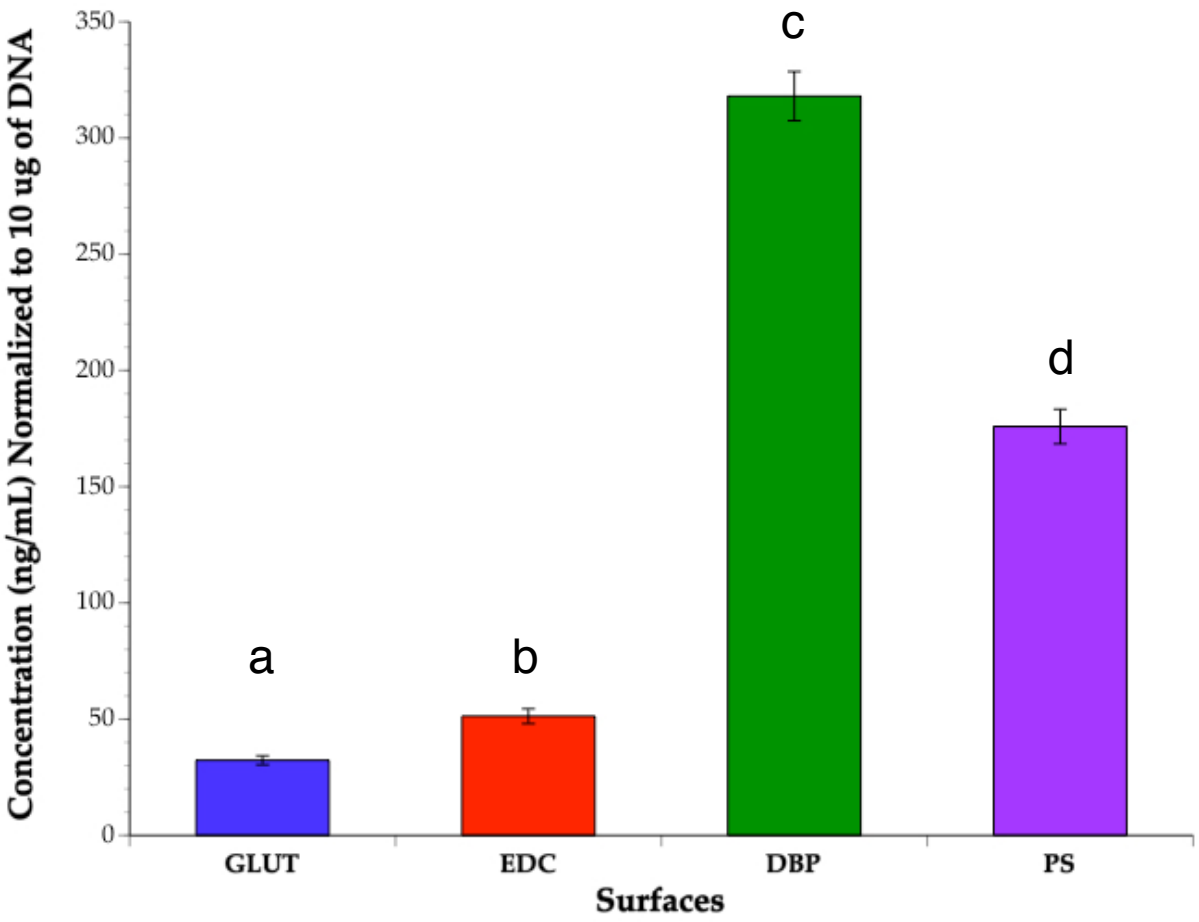

Figure 4-12: MMP-2 Released from U937 Cells

Matrix metalloproteinase 2 concentration as determined using an ELISA (ng/mL normalized to 10 μg DNA) of cell releasate after 72 h cell culture on the four surfaces. Different letters denote a significant difference from other surfaces at an overall significance level of P<0.008.

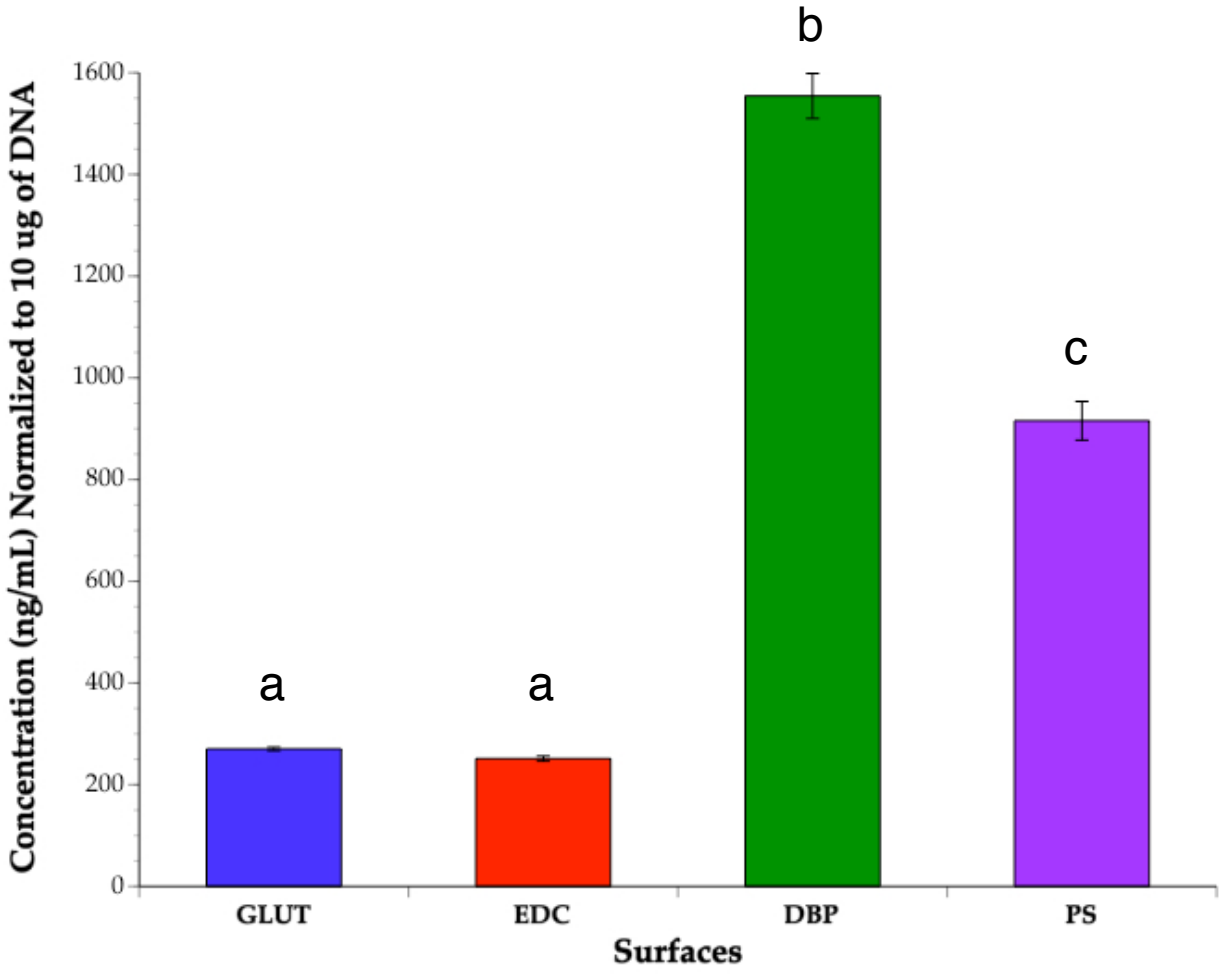

Figure 4-13: MMP-9 Released from U937 Cells

Matrix metalloproteinase 9 concentration as determined using an ELISA (ng/mL normalized to 10 μg DNA) of cell releasate after 72 h cell culture on the four surfaces. Different letters denote a significant difference from other surfaces at an overall significance level of P<0.008.

Table 4-2: Matrix Metalloproteinase Concentration Released from U937 Macrophage-like Cells on the Various Surfaces.

Surfaces	MMP-1 (pg/mL)	MMP-2 (pg/mL)	MMP-9 (pg/mL)
Untreated Decellularized Pericardial Matrix	760 ± 60	318 ± 11**	1554 ± 44†
Glutaraldehyde-treated Decellularized Pericardial Matrix	> 20,000[1]*	32 ± 2	270 ± 4
Carbodiimide-treated Decellularized Pericardial Matrix	1140 ± 140	51 ± 3	251 ± 5
Tissue Culture Polystyrene	> 20,000[1]*	176 ± 7	916 ± 38†

[1] Values determined were above the detection ceiling of the ELISA kit.
** indicates a significant difference compared to the carbodiimide-treated and untreated pericardial matrix (P = 0.008)*
*** indicates a significant difference compared to the other surfaces (P = 0.008)*
† indicates a significant difference compared to the crosslinked pericardial matrices (P = 0.008)

2 and more MMP-9 activity compared to MMP-2. The amount of intracellular MMP-1 was highly variable in the U937s on the four surfaces. The amount of released MMP-1 from the U937s on the glutaraldehyde-treated and polystyrene surfaces were generally above the detection ceiling of the kit. Despite this, U937s cultured on DBP and TCPS released greater amounts of MMP-2 and MMP-9 activity compared to cells on either crosslinked substrate.

4.4.3 Cytokine Response to Biomaterial Surface

Cells on all four surfaces, even the glutaraldehyde-damaged cells, released the cytokines IL-1Ra, IL-6, IL-10, and TNF-α (Figures 4-14, 4-15, 4-16, and 4-17, respectively). Refer to Table 4-3 for the absolute values for the released cytokines. U937 macrophage-like cells on the glutaraldehyde-treated matrix released significantly higher amounts of pro-inflammatory cytokines (IL-6 and TNF-α) compared to those on the carbodiimide-treated surface. Cells differentiated on glutaraldehyde-treated surface released lower amounts of the wound healing cytokine IL-1ra compared to the other surfaces. There was a significant difference in the release of the wound healing cytokine IL-10 between the two crosslinked surfaces but not compared to the DBP. Additionally, the glutaraldehyde-treated surface showed higher amounts of released pro-inflammatory cytokines compared with the cells on the other surfaces.

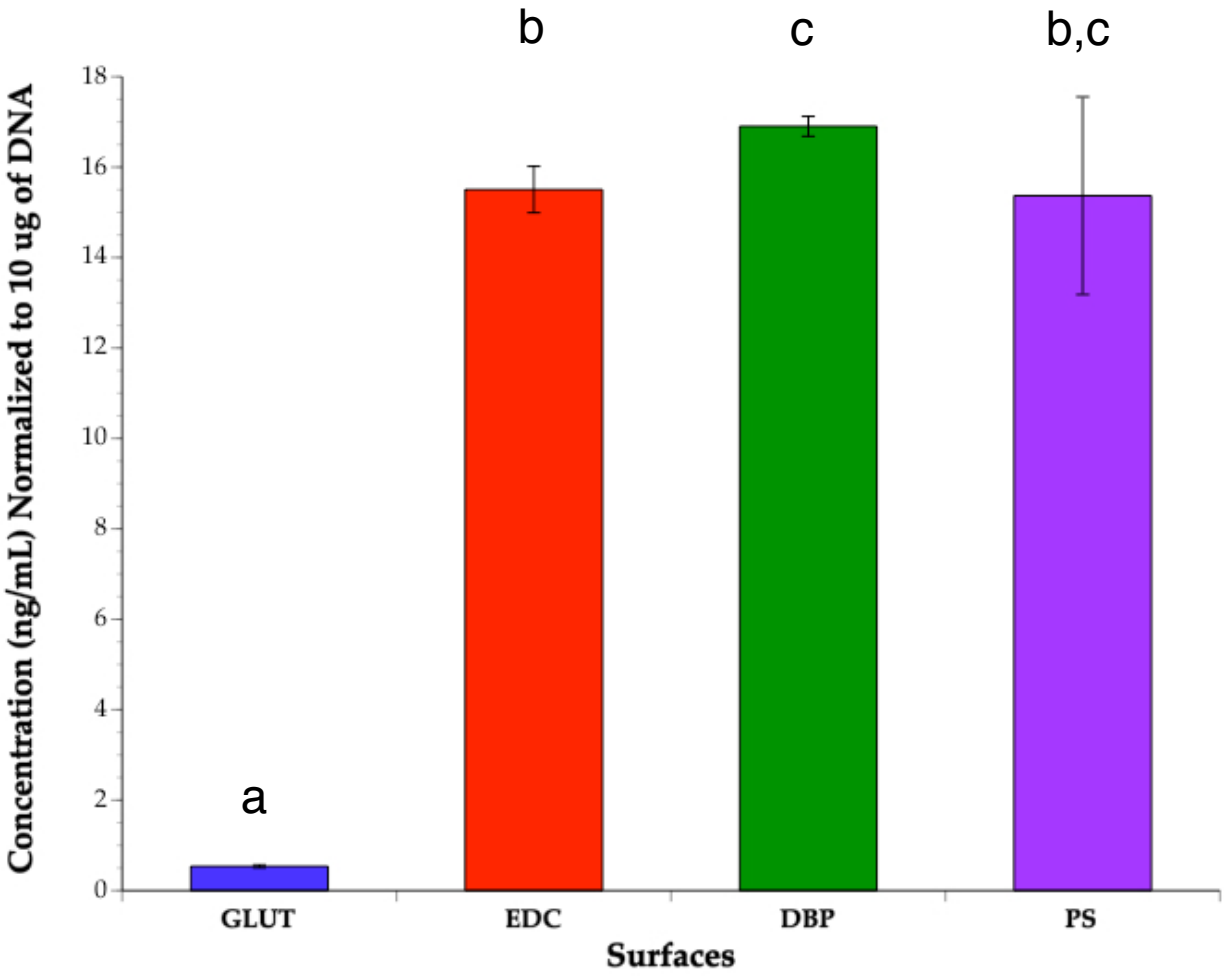

Figure 4-14: IL-1Ra Released from U937 Cells

Interleukin-1 receptor antagonist concentration as determined using an ELISA (ng/mL normalized to 10 μg DNA) of cell releasate after 72 h cell culture on the four surfaces. Different letters denote a significant difference from other surfaces at an overall significance level of P<0.008.

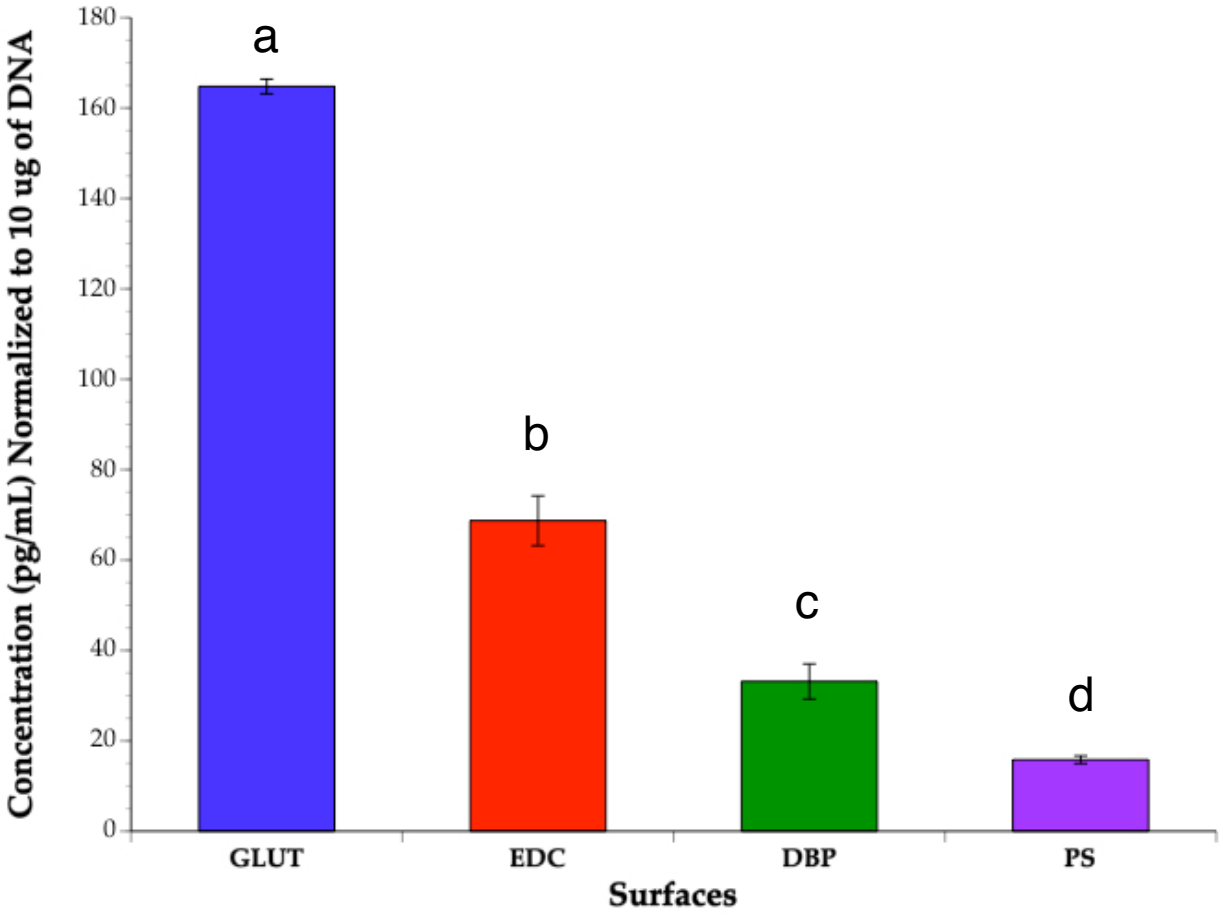

Figure 4-15: IL-6 Released from U937 Cells

Interleukin-6 concentration as determined using an ELISA (ng/mL normalized to 10 μg DNA) of cell releasate after 72 h cell culture on the four surfaces. Different letters denote a significant difference from other surfaces at an overall significance level of P<0.008.

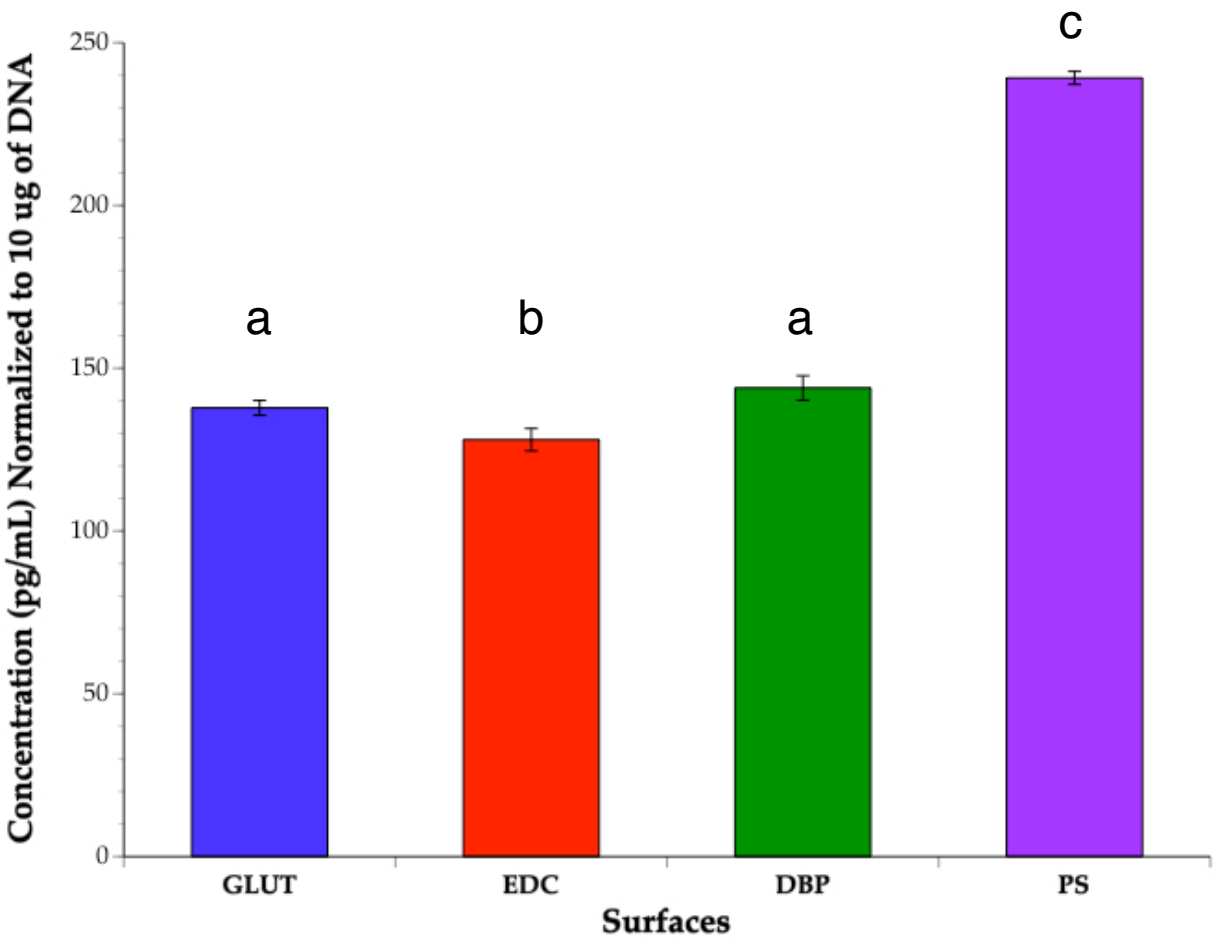

Figure 4-16: IL-10 Released from U937 Cells

Interleukin-10 concentration as determined using an ELISA (ng/mL normalized to 10 μg DNA) of cell releasate after 72 h cell culture on the four surfaces. Different letters denote a significant difference from other surfaces at an overall significance level of P<0.008.

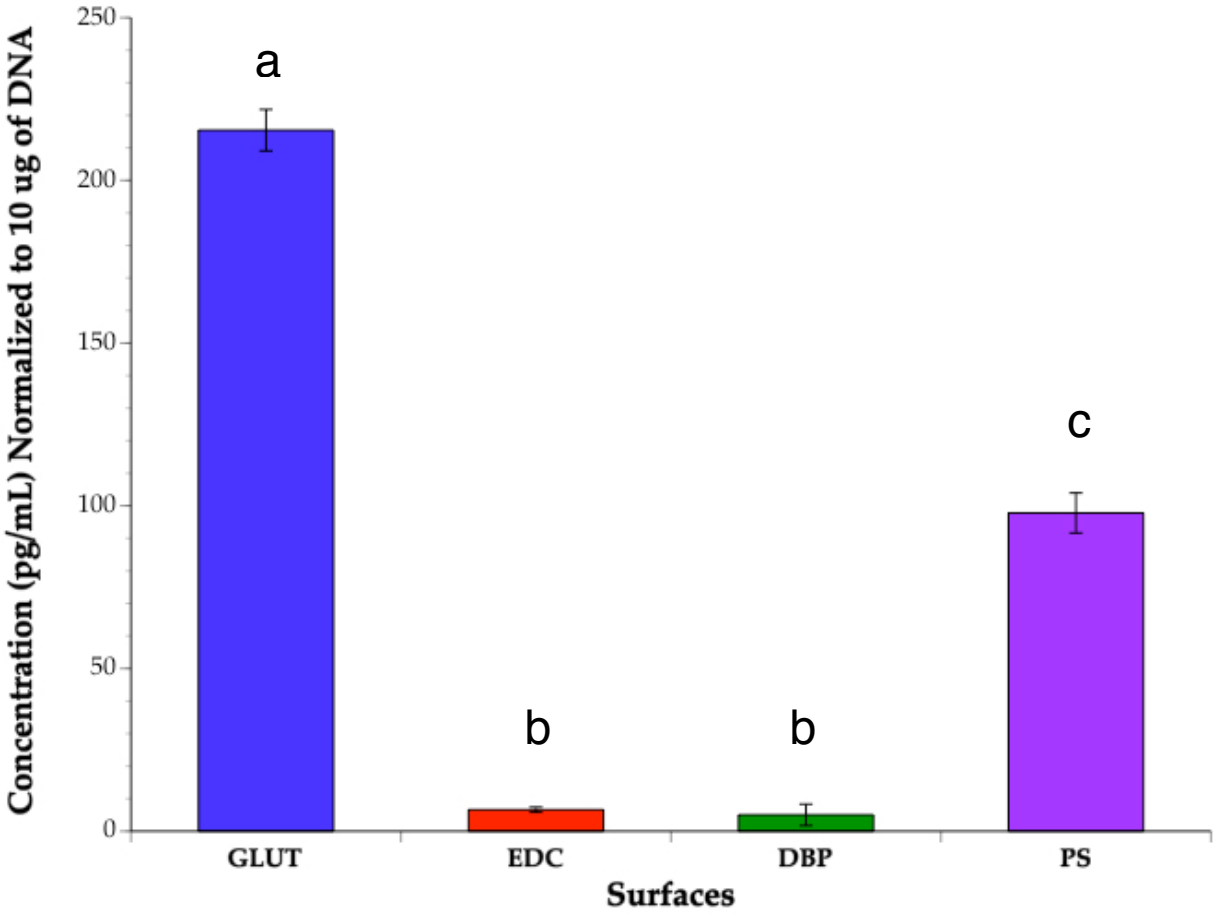

Figure 4-17: TNF-α Released from U937 Cells

Tumor necrosis factor - α concentration as determined using an ELISA (ng/mL normalized to 10 μg DNA) of cell releasate after 72 h cell culture on the four surfaces. Different letters denote a significant difference from other surfaces at an overall significance level of P<0.008.

Table 4-3: Cytokine Concentration Released from U937 Macrophage-like Cells on the Various Surfaces.

Surfaces	IL-1ra (ng/mL)	IL-6 (pg/mL)	IL-10 (pg/mL)	TNF-α (pg/mL)
Untreated Decellularized Pericardial Matrix	17 ± 0.2	33 ± 4	144 ± 4	5 ± 3
Glutaraldehyde-treated Decellularized Pericardial Matrix	0.5 ± 0.1*	165 ± 2**	138 ± 2	215 ± 6‡
Carbodiimide-treated Decellularized Pericardial Matrix	16 ± 1	69 ± 6	128 ± 4†	7 ± 1
Tissue Culture Polystyrene	15 ± 2	16 ± 1	239 ± 2†	98 ± 6‡

, indicates a significant difference compared to the other surfaces (P = 0.008)*
† indicates a significant difference compared to the glutaraldehyde-treated and untreated pericardial matrix (P = 0.008)
‡ indicates a significant difference compared to the carbodiimide-treated and untreated pericardial matrix (P = 0.008)

Chapter 5: Discussion

5.1 General Discussion

Recent work done by Ariganello *et al*.[89] was the first to investigate U937 macrophage-like cells and their interactions with decellularized bovine pericardium. From this study, the authors were able to demonstrate that the U937 cells could accurately predict the response of monocyte-derived macrophages *in vitro* to the decellularized pericardial matrix. Using macrophages that were directly differentiated on the decellularized pericardial matrix, Ariganello *et al*.[39,90] was able to better model the material effect by analyzing matrix metalloproteinase and cytokine activity.

The mounting circumstantial evidence against macrophages and their role in the failure of bioprosthetic heart valves is substantial. Macrophages have been repeatedly found on the surface of crosslinked valve surfaces and near physical disruptions in collagen fibers. The goal of this thesis was to investigate the interaction of macrophages in the failure mechanism of tissue-derived heart valves that have been chemically crosslinked by measuring their interactions and cellular response to intact collagenous materials. In all of the studies, the glutaraldehyde-treated surface exhibited the least amount of acid phosphatase, lactic acid dehydrogenase, and MMP-2 and MMP-9 activity and the lowest amount of cellular attachment compared to the alternative chemical treatment (carbodiimide) and the control surfaces (DBP and TCPS). These results provide insight towards how macrophage-like cells may respond to the future generation of tissue-engineered scaffolds for heart valve replacements. The observations made through this research were possible because of

the simplified *in vitro* system that was chosen as a model of the more complicated clinical environment. This thesis reports some of the first studies to investigate macrophage responses to crosslinked decellularized matrices. This will allow the work to look not only at tissue engineering substrates but take a look at what might be happening with failed bioprostheses.

5.1.1 Differential Scanning Calorimetry Verification of Pericardial Crosslinking

Differential scanning calorimetry (DSC) is a well developed method for study of enthalpy-associated structural changes in materials and has been used for several years in the study of collagenous biomaterial denaturation[105]. The present DSC data displayed a single asymmetrical peak corresponding to denaturation of the bovine pericardial collagen. The denaturation temperatures recorded (Table 4-1) were in accordance with the literature values ($85.3 \pm 0.4^{o}C$ and $86.0 \pm 0.3^{o}C$ for glutaraldehyde-treated and carbodiimide-treated pericardial matrix[54,105], respectively), verifying the crosslinking protocols used for the glutaraldehyde and carbodiimide treatment of the bovine pericardial samples.

5.1.2 Cellular Response to the Biomaterial Surfaces

It is well understood that macrophages play an important role at the site of implantation, associated with the degree and type of foreign body response, and with increasing importance during the chronic phase of inflammation[67]. This is espe-

cially true for heart valve replacements, which are ideally implanted for the lifetime of the patient. Still, few studies have made headway in identifying the mechanisms of the chronic response or, more specifically, the roles of macrophages on collagenous or crosslinked decellularized biomaterials. The present thesis has attempted to ascertain the physical and chemical response of the macrophage-like U937 cell line to the surface of a crosslinked decellularized, tissue-derived biomaterial suitable for a heart valve replacement.

There has been an increase in the use of decellularized tissues in regenerative medicine and tissue engineering since these scaffolds offer a relatively native matrix material that retains most of the mechanical and structural properties that are required for its function[106]. The success of the decellularization process is clearly dependent on the intensity and efficacy of the extraction protocol[107]. The decellularization process that was followed was modeled after the protocol developed by Courtman *et al.* more than fifteen years ago[40].

Due to the ease of culture, as well as the homogeneity of the cell type[76], U937 cells were used in this research to investigate the macrophage interaction with crosslinked decellularized cardiovascular biomaterials. Despite some dissimilarity between the cell line U937 and MDMs, U937s are useful in preliminary investigations of the biocompatibility of biomaterials. The work of Matheson *et al.*[76] showed that the U937 and MDM response to polyurethane biomaterials was similar in terms of enzyme secretion, degradation capacity, and protein synthesis. This provided evidence that U937s may have similar signaling pathways and hydrolytic enzyme re-

sponses as MDMs to some biomaterials. A study by Yagil-Kelmer *et al.*[108] found that U937s and MDMs also had similar secreted cytokine profiles when responding to alumina ceramic particles. Additionally, previous work has shown that U937s exposed to PMA were still responsive and sensitive to a biomaterial surface (or the protein layer adsorbed to that surface), as differences between surfaces have been found for enzyme activity, protein secretion and degradation capacity after exposure of U937s to PMA[109,110]. In a very recent study, Ariganello *et al*.[89] examined the response of human MDMs and U937s to decellularized bovine pericardium. The authors found that the MDMs closely parallel the response of U937s in terms of acid phosphatase activity and cellular morphology, despite the difference in origins of the cell types: U937s, a proliferative cell line, are derived from the pleural effusion of an acute histiocytic leukemia whereas MDMs are derived from the end-stage terminated peripheral blood monocyte[39].

Cell attachment was quite distinct on the four surfaces (Figure 4-6). A significant difference in the amount of DNA was observed between the cell populations on the glutaraldehyde-treated and carbodiimide-treated substrates. This surface-dependent difference between the crosslinked surfaces highlights the possibility of residual cytotoxic aldehyde groups or glutaraldehyde monomers leaching from the surface and into the growth media. During the glutaraldehyde fixation process, a 0.1 M glycine solution was used to quench any unreacted glutaraldehyde from the crosslinking reaction. Upon further investigation, a weak solution of glutaraldehyde with increasing concentrations of glycine buffer (up to 0.1 M) was analyzed spectrophotometrically with a UV/Vis spectrophotometer (Helios series, Geneq, Montreal

Canada). This experiment was performed to assess the efficiency of the glycine solution at reacting with unreacted aldehyde groups. Comparing the spectra of unreacted glutaraldehyde to that of the glutaraldehyde and glycine solution, no significant differences in the spectra were detected. This suggests that the subsequent glycine washes following glutaraldehyde crosslinking was not efficient in the removal of unreacted aldehydes. There is also the possibility of glutaraldehyde release due to the dissociation of the unstable Schiff-base bond that links the aldehyde moieties of glutaraldehyde to the amines of the tissue[50,111,112]. Adding to that point, the glutaraldehyde polymers may depolymerize, as well as the reversal of unstable crosslinks that are formed, both of which result in cytotoxic glutaraldehyde monomers in solution. In contrast, the crosslinking reaction using carbodiimide (Figure 1-2) forms peptide bonds instead of chemical crosslinks and produces a nontoxic by-product, urea. This alternative to glutaraldehyde-fixation would not be expected to disrupt cellular viability since the peptide crosslinks in the tissue are amide bonds which are more stable than initial Schiff-base bonds formed by glutaraldehyde, thereby reducing the risk of degeneration[92].

In addition to the significant difference in cellular attachment between the crosslinked surfaces, the amount of DNA on the tissue culture polystyrene differed significantly compared to that on the glutaraldehyde-treated matrix. As the control surface, TCPS is universally used for cell culture. The macrophage-like cells cultured on the TCPS had the highest attachment on this material. However, recent studies have demonstrated that a tissue culture polystyrene surface is activating to U937 cells[113]. Similarly, TCPS has been shown to be an activating surface for macro-

phages[114]. It is especially interesting then that, when compared to this activating surface, the uncrosslinked DBP surface was less stimulating (Figure 4-9 and 4-10), as measured by the acid phosphatase profiles. The increased intracellular enzyme content of cells cultured on TCPS demonstrated that these cells were synthesizing more protein, although further investigation is needed to fully profile the specific intracellular protein differences that resulted from the culture surfaces.

Acid phosphatase was chosen because it is a lysosomal enzyme, providing an implicit measurement of lysosomal enzyme secretion. Further, it is a marker for the innate immune response and cellular activation[115]. Cells cultured on glutaraldehyde- and carbodiimide-treated surfaces (after differentiation for 72 h) released lower amounts of acid phosphatase activity compared to cells cultured on the DBP and TCPS. On the crosslinked surfaces, there was a significant difference in the amount of released acid phosphatase activity on the glutaraldehyde-treated pericardial matrix compared to the carbodiimide-treated surface (Figure 4-10). If the total acid phosphatase activity is compared, the macrophage-like U937 cells synthesized significantly less enzyme on the glutaraldehyde-treated surface than did cells on the other surfaces. This implies a less activated cell type and that there may be cytotoxicity issues with the glutaraldehyde fixation. Glutaraldehyde from the crosslinked surface could be affecting the cells such that their protein synthesis is significantly decreased or inhibited. During the cell cycle, specifically the G_2 phase, significant protein synthesis occurs, which is a requirement for mitosis. If their growth rate while cultured on the glutaraldehyde-fixed pericardium is affected, then the subsequent protein synthesis levels would be decreased as a result.

5.1.3 Lactic Acid Dehydrogenase Activity in Response to the Biomaterial Surfaces

The total lactic acid dehydrogenase (LDH) activity (Figure 4-8) from cells on the glutaraldehyde-fixed surface was significantly different when compared to the other surfaces. The LDH activity assay measures the production of lactate from pyruvate by measuring the disappearance of pyruvate. If there are high levels of pyruvate, then the corresponding LDH enzyme activity is low[101]. LDH is a cytosolic enzyme and therefore its activity should not be detected in the releasate of the U937 macrophage-like cell. Measurable amounts of activity in the releasate therefore is an indication of compromised cellular membranes[101]. Comparing the micrographs of the U937s cultured on the various surfaces (Figures 4-2 to 4-5), in particular those cells on the glutaraldehyde-fixed surface, a very different cellular morphology is evident there. The extracellular membrane appears severely degraded or destroyed when compared to the cells on the remaining surfaces. Although it would seem that cells on the glutaraldehyde-fixed surface are non-viable, structurally they maintain their shape whereas a necrotic cell would not have a distinct cellular shape. Curiously, despite the cellular morphology on the glutaraldehyde-fixed surface, there *is* protein synthesis occurring, as demonstrated in Figures 4-7 and 4-8.

There is one particular aspect of the LDH activity produced by the cells on the various surfaces that should be consistent amongst the different substrates. The total LDH activity, combining what is released from the cells with the intracellular activity, should be complementary. That is, when referenced to DNA content, the cells on the four surfaces should synthesize similar amounts of total LDH. This is not the

case, however. There is significantly less total activity from the cells on the glutaraldehyde-fixed surface (approximate 80% loss of activity). This observation can be related back to the overall decrease in protein synthesis as a result of cytotoxicity from the glutaraldehyde. Another interesting point with the LDH activity, in particular the activity found in the cellular *releasate*, is the significantly higher levels detected from the cells on the glutaraldehyde-treated surface. As previously mentioned, detectable activity in the cellular releasate indicates compromised cell membranes. Knowing this, and referring back to the micrographs of the cells on the glutaraldehyde-treated surface (Figure 4-2), the observed cellular morphology corresponds well. The cell membranes appear degraded or destroyed, allowing for the intracellular contents to be released, including enzymes such as LDH and acid phosphatase.

5.1.4 Macrophage-like Cell Viability

Assessing cell viability on the four surfaces can be accomplished in several ways. In the present thesis, assays for lactic acid dehydrogenase activity and DNA content were performed (Figures 4-6 and 4-7). Once a U937 cell is differentiated into a macrophage-like cell using PMA, it stops proliferating and attaches to the material surface. In the case of the glutaraldehyde-treated substrate, the overall cell attachment and lactic acid dehydrogenase activity were significantly less compared to cells on the other surfaces. At first glance, one would think that the residual glutaraldehyde monomers/polymers in solution or leached glutaraldehyde from the matrix would be killing the cells; however, if a cell is dead then it would not transcribe and

ultimately produce enzymes, as seen with detectable lactic acid dehydrogenase activity intracellularly (Figure 4-7). It could be hypothesized that the glutaraldehyde is cytotoxic to the cells affecting their attachment and cellular performance but not killing them. However, another possibility exists that the residual glutaraldehyde in solution could have crosslinked dead cells to the surfaces and the DNA measured was that of a dead cell.

Additionally, cell viability can be measured using the MTT assay which involves the conversion of MTT (3-[4,5-Dimethylthiazol-2-yl]-2,5-diphenyltetrazolium bromide) into an insoluble formazan dye. Viable cells reduce the MTT reagent to a coloured product using the enzyme succinate dehydrogenase[116]. Cells that were non viable or lacking the necessary enzyme would not be able to convert the reagent into the detectable colour dye.

5.1.5 Matrix Metalloproteinase and Cytokine Release

The action of matrix metalloproteinases (MMPs) was originally believed to be restricted to degradation of the extracellular matrix. These enzymes can degrade all components of the extracellular matrix, thereby influencing many important processes such as cell proliferation, differentiation, migration, and death[117]. It is therefore not surprising that MMPs play an important role in many physiological processes and also in many pathological conditions such as cancer invasion, arthritis, and atherosclerosis[118]. The role of MMPs has been made even more complex by the increasing number of studies revealing many non-matrix substrates such as chemoki-

nes, cytokines, and growth factors, indicating that MMPs influence an even wider array of physiological and pathological processes[118,119].

The release of both MMP-2 and MMP-9 on all surfaces (Figures 4-12 and 4-13) does not necessarily imply a degradative response to the biomaterial surface because gelatinases play important roles in both immune and inflammatory responses (by processing cytokines and chemokines) in addition to matrix or protein proteolysis[118,120,121]. More specifically, a recent study of differentiated macrophages demonstrated that MMP-9 secretion may be a marker of wound healing macrophages[122] . The study by Lolmede *et al*.[122] found that MMP-9 was secreted only from macrophages that were polarized towards a wound healing phenotype (previously exposed to IL-4 or IL-10), not by macrophages polarized towards an inflammatory phenotype. Referring to Figure 4-12, it is interesting that the low release of MMP-2 was affected by the substrate (crosslinked surfaces compared to the controls), while the greater release of MMP-9 (Figure 4-13) was surface dependent. Previous studies of gelatinase release from macrophages on biomaterial surfaces have similarly found that the release of MMP-9 was at least one order of magnitude greater than the release of MMP-2, but have not been able to demonstrate that the release of one or the other gelatinase is more surface dependent [123,124]. Very recent work by Ariganello *et al*.[90] investigated the release of MMP-2 and MMP-9 from MDMs on decellularized bovine pericardium and two polymer control surfaces. For every surface, significantly more MMP-9 activity was released compared to MMP-2 activity. The study by Schmidt *et al*.[124] concluded that the release of MMP-2 from macrophages did not

change on a variety of surfaces, although there was a 30% lower MMP-2 release on TCPS compared to a polyethylene glycol hydrogel after only 7 d in culture.

Early studies by Simionescu *et al* [37,125]. reported the presence of MMPs in diseased human valves and in bioprostheses made of glutaraldehyde-treated bovine pericardium. These MMPs have been associated with, but not proven to be, the cause of early degradation and degeneration of tissue-derived bioprostheses. In a similar study, Calero *et al*.[126] showed that calf and pig pericardium contained gelatinolytic activities (MMP-2 and MMP-9) and suggested that these enzymes may be partially responsible for the degradation of pericardium-based biomaterials after *in vivo* implantation[126]. Interestingly, crosslinking the tissues with glutaraldehyde or diphenylphosphorylazide almost completely abolished the gelatinase activity. Crosslinking with carbodiimide also significantly reduces gelatinase activity - but not to the extent that glutaraldehyde did[126]. Referring to Figures 4-12 and 4-13, it is likely that glutaraldehyde treatment inactivates MMPs by decreasing cell function. The concentration of MMP-2 and 9 released from cells on the glutaraldehyde-treated tissue was significantly lower than on the untreated pericardial and polymer controls. This trend was observed on the carbodiimide-treated surfaces as well. There was a significant difference in the concentration of MMP-2 released between the crosslinked surfaces, but this was not observed for the MMP-9. It is important to note that in this study by Calero *et al*.[126] and work by Ariganello *et al*.[90], the activity of the MMPs was measured using gelatin zymography. It does not directly compare to the present work, however, since zymography measures activity whereas an

ELISA measures the amount of enzyme. An ELISA can measure the inactive form of an enzyme, therefore, enzyme activity can not be determined using an ELISA or Western Blot. With the low observed concentrations of MMP-2 and MMP-9, the corresponding activity levels would be low as well.

Recent work by Schmidt *et al*.[124] looked at monocyte activation in response to polyethylene glycol hydrogels using standard tissue culture polystyrene as a control surface. Specifically, the pro-inflammatory cytokine TNF-α and the gelatinase MMP-2 and 9 concentrations were measured using an ELISA. The data for MMP-2 and 9 reported by Schmidt showed a significant difference in the concentration of MMP-9 compared to MMP-2 with a higher concentration of MMP-9[124]. This finding supports the MMP-2 and 9 data presented in Figures 4-12 and 4-13 and while the absolute values do not compare, the trends of higher concentration for MMP-9 contrast to MMP-2 matches. In the present thesis, the macrophage-like cells were cultured for 72 h on the polystyrene before the amount of the MMPs was measured. In contrast, Schmidt and co-workers cultured the monocyte-derived macrophages for 24 or 96 h, however; no significant difference in concentration was observed between these time points[124].

In a similar study, Chung *et al*.[127] investigated MMP-2 and 9 concentrations from monocyte-derived macrophages on polystyrene and a glutaraldehyde-fixed gelatin hydrogel. Similar to the present thesis, the determined concentration of MMP-9 was significantly lower than that of MMP-2 for the macrophages cultured on the polystyrene compared to the glutaraldehyde-treated gelatin[127]. Macrophages on

the glutaraldehyde-treated hydrogel followed the same trend as the cells on the polystyrene did, however; the determined concentrations were significantly lower than those observed for the macrophages on the polystyrene. Again, the culture time points mirrored those of Schmidt *et al*.[124] and no significant difference was observed between the two. Despite the differences between the glutaraldehyde-treated hydrogel used in the work by Chung[127] and the glutaraldehyde-treated decellularized pericardium used in the present work, the trends of lower MMP-2 and 9 concentrations compared to the macrophages cultured on the polystyrene control are comparable.

MMPs are secreted by both inflammatory and stromal cells in response to inflammatory cytokines such as TNF-α[117]. MMP secretion is down-regulated by cytokines including IL-4 and IL-10[128], although the regulation of secretion is cell- and stimulus-specific. When the host immune system is challenged by an invading organism, it must first recruit leukocytes to the site of infection, eradicate the pathogen, and then reduce the response to allow the resolution of inflammation. MMPs play an important role in this process, both by degrading components of the extracellular matrix and by modulating cytokine and chemokine activity[117]. The migration of immune cells from the blood stream to sites of inflammation requires proteolysis of the basement membrane. In addition to opening a path through the ECM for cell migration, MMPs modulate the chemokine and cytokine gradients that drive inflammatory cell recruitment[117]. MMP-1, 2, 3, 7, 9 and 12 can release active TNF-α

from the membrane-anchored precursor by a similar mechanism to TNF-α converting enzyme[117,118].

The higher concentration of the collagenase MMP-1 released from U937s on the glutaraldehyde-treated and polystyrene surfaces was unexpected. In a study by Cheung and Nimni[51], they hypothesized that glutaraldehyde coats collagen fibers by producing a polymer semi-plastic coating that inhibits further penetration into the tissue. Perhaps this semi-plastic coating that the macrophage-like cells adhere to and interact with is similar to the polystyrene surface that the cells interact with. This could explain the similarity in the release of MMP-1 protein from U937s on the glutaraldehyde-treated and polystyrene surfaces. By contrast, neither the carbodiimide nor the untreated pericardium were great activators of MMP-1 release. Additional indirect evidence for low, active MMP-1 release may be the lack of cell penetration into the collagen matrix seen in the SEM images (Figures 4-2 to 4-5). The relatively dense collagen network would require local collagen disruption for U937s to migrate into the matrix.

Macrophages at an implant surface are derived from monocytes that encounter molecular signals as they migrate into the tissue from the vasculature. These macrophages interact with the material and secrete an array of cytokines, chemokines, and growth factors to direct the foreign body reaction[129]. Pro-inflammatory cytokines, such as TNF-α and IL-8, recruit immune cells such as monocytes to the implant site to promote inflammation whereas anti-inflammatory cytokines like IL-10 and IL-1ra suppress pro-inflammatory signals in order to down-regulate inflammation[129]. IL-10

down-regulates transcription of many pro-inflammatory cytokines through the inhibition of nuclear factor kappa B (NFκB) transcription[130].

In this thesis, levels of IL-1ra, IL-10, IL-6, and TNF-α released from U937 macrophage-like cells were measured as markers of an inflammatory or wound healing polarization in these cells (Figures 4-14 to 4-17). The TNF -α and IL-6 released from U937s on the glutaraldehyde-treated surface was significantly higher compared to that of cells on the other surfaces. In a recent study by Bayrak *et al*.[131] the released TNF -α and IL-6 from human peripheral blood mononuclear cells (PBMCs) on glutaraldehyde-treated porcine matrix were measured. After five days of culture, the concentrations of released TNF-α and IL-6 were significantly higher than that for IL-10[131]. This is in line with the data obtained in the present thesis, showing that cells cultured on the glutaraldehyde-treated surface released more pro-inflammatory cytokines compared to cells on the other surfaces where the concentration of released anti-inflammatory cytokines (IL-1ra and IL-10) was significantly lower. For reference, one should note that a study conducted by Mocellin *et al.*[132] showed that IL-10 is a pleiotropic cytokine and, although it is generally considered an immunosuppressive molecule, it has immunostimulatory properties. They suggested that these contrasting effects are dependent upon experimental conditions, the immune effector mediating the given immune response, timing of IL-10 production, and the dose and/or location of expression[132].

The final differences in cytokine expression that were found in this thesis were in extracellular cytokine release. Substrate differences were identified; however,

overall the cytokine release was quite low. Of all the cytokines measured, only one had a concentration within the ng/mL range: IL-1ra (on all surfaces except for glutaraldehyde-treated). IL-1ra is an antagonist for the IL-1 receptor, which inhibits IL-1 induced cytokine synthesis[73]. In a very recent study by Ariganello *et al*.[90] the gene expression of IL-1ra was increased after exposure to amphotericin B, which was used in the culture media, which could possibly explain why IL-1ra was elevated in general, but does not explain the differential release on each substrate.

The concentration of cytokines seen in the present thesis can be considered to be low because a recent study showed higher amounts of cytokines released (on the order of ng/mL)[129]. Schutte *et al*.[129] looked at cytokine release from THP-1 cells after PMA differentiation (an alternative model of macrophage activation and differentiation). Compared to the cytokine expression from the PMA-treated THP-1 cells, the U937s generated in this direct differentiation model consistently released lower levels of all cytokines. Another *in vitro* study similarly looked at cytokine release during the course of differentiation of human monocytes on various polymers[133]. The MDMs on all surfaces in that study released greater amounts of cytokines than were released from U937 macrophage-like cells on the various surfaces in the present thesis. It is difficult to ascertain, in general, whether statistically different levels of cytokines released *in vitro* have any physiological significance and whether cytokine levels used to stimulate cell behaviour *in vitro* are similar to the concentration required *in vivo*. As well, 1 pg/mL of IL-1ra, for example, may not be equivalent in terms of effect to 1 pg/mL of IL-10.

It was attempted in this thesis to characterize the U937 macrophage-like cell phenotype on each of the four surfaces in terms of polarization. However, the goal of establishing U937 polarization may have simply been too ambitious for one particular reason. An *in vitro*, single-cell culture system model lacks alternative cell types (e.g. lymphocytes) and their associated cytokines, (e.g. IL-4, IL-13, INF-γ), which are the classical inducers of M1/M2 phenotypes[80]. It may be impossible for such a simple *in vitro* culture system to adequately predict the U937 macrophage-like phenotype that would develop *in vivo* in response to a biomaterial.

5.2 Significance

This thesis represents the first studies to directly investigate how macrophage-like cells interact with crosslinked decellularized scaffolds. This is significant given the importance of macrophage responses in the determination of a biomaterial's biological performance *in vivo*. The work done in this thesis cannot directly relate to failed bioprosthetic heart valves or tissue engineering since the scaffold used does not truly represent what the current generation of replacement heart valves are constructed of. The use of a decellularized matrix represents a collagen source free of cells and cellular debris. The addition of glutaraldehyde and carbodiimide crosslinking to the collagen scaffold allows for the investigation of the crosslinking affects on the cellular response to collagen without the complexity of the variables present *in vivo*. Therefore this simplified *in vitro* model of macrophage interactions with crosslinked decellularized scaffolds could be predictive of the response that a representative crosslinked heart valve replacement could elicit. While the conclusions

drawn throughout this thesis are not completely relevant to clinically available replacement heart valves, the macrophage interactions to the crosslinked surfaces represents the first study of its kind to investigate the direct differentiation of macrophage-like cells on crosslinked decellularized matrices.

This thesis also attempted to demonstrate the predictive power of U937 macrophage-like cell characterization for implantation studies. Macrophages play contrasting functions in the body and it is important that these functions are defined in scientific studies when predicting or concluding a biomaterials' biocompatibility. The results of current research demonstrated that macrophage-like cells on glutaraldehyde-treated decellularized bovine pericardium have altered membrane morphology, decreased cellular attachment and enzyme activity, and an increased release of pro-inflammatory cytokines when compared to carbodiimide-treated and the untreated control substrates. These results provide evidence that crosslinking with glutaraldehyde is cytotoxic to the cells, either through depolymerization of the glutaraldehyde polymers, leaching of absorbed/adsorbed glutaraldehyde, or the reversal of unstable crosslinks, and that the amide crosslinking with carbodiimide can be viewed as the alternative to glutaraldehyde fixation. It is important to note that the technology of crosslinking biomaterials with carbodiimide has been around for almost fifteen years, described by several research groups in the early 1990s[54,56,62,92], with a patent for carbodiimide fixation of biological tissue filed by Girardot and Girardot in 1995[134]. Despite this early research effort, to the author's knowledge, *in vivo* implantation of a collagenous biological matrix crosslinked with carbodiimide has not been examined in detail and no commercial surgical product has emerged. Per-

haps there is an issue with carbodiimide stabilization *in vivo*. Since the mechanism of crosslinking with carbodiimide involves the formation of peptide bonds, there may exist a nonspecific enzyme that cleaves peptide bonds, thus cleaving the crosslinks. While it is hoped that, with greater sophistication and validation, such *in vitro* models of biomaterial crosslinking with carbodiimide may help with *in vivo* implantation. Nonetheless, it remains likely that crosslinking with glutaraldehyde, despite the issues of cytotoxicity observed in the present thesis, will carry on as being the primary pre-implantation fixation method - at least until tissue engineering of valve replacements becomes commercially practical.

5.3 Summary

In summary, the results of the present study suggest that U937 macrophage-like cells differentiated and cultured on glutaraldehyde-treated decellularized bovine pericardial matrix are not as active as cells on carbodiimide-treated and the untreated control substrates. This was demonstrated with significantly lower amounts of released and intracellular acid phosphatase activity as well as an approximate 80% loss of lactic acid dehydrogenase activity.

We hypothesized that, U937 macrophage-like cells seeded onto the glutaraldehyde-treated pericardial tissue would be morphologically different than cells seeded onto the carbodiimide-treated and control tissues. This was certainly confirmed. The extracellular membranes of the cells were severely degraded and/or destroyed, while cells on the other surfaces appeared healthy. The degraded or leaky

membranes corresponded with the increase in released lactic acid dehydrogenase activity seen from the U937s on the glutaraldehyde-treated pericardium. Adding to that point, we hypothesized that the quantity of U937 macrophage-like cells adherent on the glutaraldehyde-treated pericardial tissue would be significantly less compared to the carbodiimide-treated or control tissues. Continuing from the results from the first hypothesis, the number of U937 cells on the glutaraldehyde-treated surface was significantly less. Furthermore, there was a significant difference in adherence between the two crosslinked surfaces, suggesting that the glutaraldehyde-treatment is more cytotoxic to the cells or it inhibits cellular attachment. Finally, we set out to determine if U937 macrophage-like cells on the untreated decellularized bovine pericardium released less pro-inflammatory cytokines, when compared to the two crosslinked surfaces: in other words, the crosslinked pericardial surfaces would be more inflammatory, while the untreated pericardial substrate would be immunosuppressive. Analyzing the concentration of released cytokines from the macrophage-like cells on the test substrates, cells on the two crosslinked surfaces released a significantly higher concentration of pro-inflammatory cytokines compared to the untreated surfaces. Furthermore, cells on the glutaraldehyde-treated surface elicited more of an inflammatory response, releasing a significantly higher concentration of pro-inflammatory cytokines compared to the carbodiimide-treated substrate.

5.4 Limitations and Suggestions for Future Work

For the research presented in this thesis, the immortal cell line U937 was used. The primary disadvantage of such a cell line is that it does not represent a physiologically normal, typical macrophage, and therefore the results may be misleading or clinically irrelevant[88]. Despite the heterogeneity and the variation between human donors, as well as the lengthy culturing protocols, primary cells derived from humans remain the preferred cell source to use in studying biomaterial interactions. The present simplified approach was selected for the experimentation throughout this thesis, as it would initially provide a more controlled study that could be expanded upon and enhanced by future investigators.

Further limitations existed in this single-cell model system. Aside from the lack of other cell signals and cell components such as plasma proteins, only one time point for differentiated U937s was investigated (72 h). This is a relatively early time point for implants that are designed to last for 30 years. This can be compared to the snapshot explant studies. The measured releasate from the cells was everything up to the 72 h time point while the lysate was everything that remained within the cell for 72 h. The time sequence of events over the three days was unknown. The response of U937s or other cells to a given stimulus is not static, and different genes are likely expressed from early to later exposure of a stimulus[135]. Longer-term cultures, likely co-culture systems with fibroblast or lymphocytes, will be required to determine whether the response of macrophages changes over time. This temporal limitation is especially a concern for the cytokine analysis, since cytokine release is often a time-specific process (e.g. IL-1 is considered an early inflammatory cytokine).

Thus cytokine analysis at a single time point may not be truly representative of the overall U937 response to the material[136]. Finally, the static nature of the model system used in this research does not recreate the shear forces and fluid flow experienced by heart valve replacements *in situ*. It is uncertain whether flow would alter U937 phenotype, resulting in greater attachment and activation, or if it would result in decreased cell attachment, as shown in monocytes adhering to polyurethanes[137]. However, since decellularized matrices are devoid of endothelial cells, it is unclear how attachment of macrophages to such a matrix will be affected by shear stresses. Future investigators may want to incorporate such fluid dynamics into their model systems.

It was demonstrated that the glycine wash, part of the glutaraldehyde crosslinking protocol, was not efficient in the removal of unreacted aldehyde groups from solution. Further investigation through the use of UV/Vis spectroscopy or perhaps Fourier Transform Infrared (FTIR) Spectroscopy could be performed to understand if the glycine washes are necessary during the glutaraldehyde crosslinking protocol as well as deduce the role glycine plays in quenching the unreacted aldehyde groups or glutaraldehyde monomers.

Another experiment that would assess the cytotoxicity of the residual glutaraldehyde monomers in solution would be to analyze the cell culture media. After 72 h incubation with glutaraldehyde-treated decellularized pericardial matrix, the media would be removed and used as medium for differentiating U937 cells on untreated pericardial matrix for three days. Following differentiation, the macrophage-like cells would undergo SEM and DNA analysis to understand the extent of the cy-

totoxic effects the glutaraldehyde monomer or polymer in the incubation solution have on the U937 macrophage-like cells.

References

1. Yacoub MH, Takkenberg JJ. Will heart valve tissue engineering change the world? Nature Clinical Practice Cardiovascular Medicine 2005;2(2):60-1.

2. Schoen FJ, Fernandez J, Gonzalez-Lavin L, Cernaianu A. Causes of failure and pathologic findings in surgically removed Ionescu-Shiley standard bovine pericardial heart valve bioprostheses: emphasis on progressive structural deterioration. Circulation 1987;76(3):618-27.

3. Implantation Biology: The Host Response and Biomedical Devices. New Jersey: CRC Press Inc.

4. Ishihara T, Ferrans VJ, Boyce SW, Jones M, Roberts WC. Structure and classification of cuspal tears and perforations in porcine bioprosthetic cardiac valves implanted in patients. Am J Cardiol 1981;48(4):665-78.

5. Ishihara T, Ferrans VJ, Jones M, Boyce SW, Roberts WC. Structure of bovine parietal pericardium and of unimplanted Ionescu-Shiley pericardial valvular bioprostheses. J Thorac Cardiovasc Surg 1981;81(5):747-57.

6. Nistal F, Garcia-Martinez V, Fernandez D, Artinano E, Mazorra F, Gallo I. Degenerative pathologic findings after long-term implantation of bovine pericardial bioprosthetic heart valves. J Thorac Cardiovasc Surg 1988;96(4):642-51.

7. Schoen FJ LR. Tissue Heart Valves: Current Challenges and Future Research Perspectives. Journal of Biomedical Materials Research 1999;47(4):439-65.

8. Lee JM, Boughner, D.R. . Bioprosthetic heart valves - Tissue Mechanics and Implications for Design. Chapter 10. In: Blood Compatible Material and Devices 1991;Technomic Pub. Co. Inc., USA.

9. Grabenwoger M, Grimm M, Eybl E, Kadletz M, Havel M, Kostler P, Plenk H, Bock P, Wolner E. New aspects of the degeneration of bioprosthetic heart valves after long-term implantation. J Thorac Cardiovasc Surg 1992;104(1):14-21.

10. Vesely I. The evolution of bioprosthetic heart valve design and its impact on durability. Cardiovasc Pathol 2003;12(5):277-86.

11. Schoen FJ. Future directions in tissue heart valves: impact of recent insights from biology and pathology. J Heart Valve Dis 1999;8(4):350-8.

12. Shaddy RE, Hawkins JA. Immunology and failure of valved allografts in children. Ann Thorac Surg 2002;74(4):1271-5.

13. Elkins RC. Is tissue-engineered heart valve replacement clinically applicable? Curr Cardiol Rep 2003;5(2):125-8.

14. Schoen FJ. Future directions in tissue heart valves: impact of recent insights from biology and pathology. Journal of Heart Valve Disease 1999;8(4):350-8.

15. da Costa FD, Dohmen PM, Duarte D, von Glenn C, Lopes SV, Filho HH, da Costa MB, Konertz W. Immunological and echocardiographic evaluation of decellularized versus cryopreserved allografts during the Ross operation. European journal of cardio-thoracic surgery : official journal of the European Association for Cardio-thoracic Surgery 2005;27(4):572-8.

16. da Costa ML, Ghofaili FA, Oakley RM. Allograft tissue for use in valve replacement. Cell Tissue Banking 2006;7(4):337-48.

17. Kidane A, Burriesci G, Cornejo P, Dooley A, Sarkar S, Bonhoeffer P, Edirisinghe M, Seifalian A. Current developments and future prospects for heart valve replacement therapy. J Biomed Mater Res Part B Appl Biomater 2009;88(1):290-303.

18. Golomb G, Schoen FJ, Smith MS, Linden J, Dixon M, Levy RJ. The role of glutaraldehyde-induced cross-links in calcification of bovine pericardium used in cardiac valve bioprostheses. Am J Pathol 1987;127(1):122-30.

19. Santini F, Luciani GB, Restivo S, Casali G, Pessotto R, Bertolini P, Rossi A, Mazzucco A. Over twenty-year follow-up of the standard Hancock porcine bioprosthesis implanted in the mitral position. Ann Thorac Surg 2001;71(5 Suppl):S232-5.

20. Marchand MA, Aupart MR, Norton R, Goldsmith IR, Pelletier LC, Pellerin M, Dubiel T, Daenen WJ, Herijgers P, Casselman FP and others. Fifteen-year experience with the mitral Carpentier-Edwards PERIMOUNT pericardial bioprosthesis. Ann Thorac Surg 2001;71(5 Suppl):S236-9.

21. Fisher J, Wheatley DJ. An improved pericardial bioprosthetic heart valve. Design and laboratory evaluation. European journal of cardio-thoracic surgery :

official journal of the European Association for Cardio-thoracic Surgery 1987;1(2):71-9.

22. Walley VM, Keon WJ. Patterns of failure in Ionescu-Shiley bovine pericardial bioprosthetic valves. J Thorac Cardiovasc Surg 1987;93(6):925-33.

23. Grunkemeier GL, Starr A, Rahimtoola SH. Prosthetic heart valve performance: long-term follow-up. Current problems in cardiology 1992;17(6):329-406.

24. Aupart MR, Sirinelli AL, Diemont FF, Meurisse YA, Dreyfus XB, Marchand MA. The last generation of pericardial valves in the aortic position: ten-year follow-up in 589 patients. Ann Thorac Surg 1996;61(2):615-20.

25. Roselli EE, Smedira NG, Blackstone EH. Failure modes of the Carpentier-Edwards pericardial bioprosthesis in the aortic position. J Heart Valve Dis 2006;15(3):421-7; discussion 427-8.

26. Schoen FJ, Levy RJ. Calcification of tissue heart valve substitutes: progress toward understanding and prevention. Ann Thorac Surg 2005;79(3):1072-80.

27. Grabenwoger M, Fitzal F, Gross C, Hutschala D, Bock P, Brucke P, Wolner E. Different modes of degeneration in autologous and heterologous heart valve prostheses. Journal of Heart Valve Disease 2000;9(1):104-9; discussion 110-1.

28. Gabbay S, Kadam P, Factor S, Cheung TK. Do heart valve bioprostheses degenerate for metabolic or mechanical reasons? J Thorac Cardiovasc Surg 1988;95(2):208-15.

29. Christie GW. Computer modelling of bioprosthetic heart valves. European journal of cardio-thoracic surgery : official journal of the European Association for Cardio-thoracic Surgery 1992;6 Suppl 1:S95-100; discussion S101.

30. Christie GW, Barratt-Boyes BG. On stress reduction in bioprosthetic heart valve leaflets by the use of a flexible stent. Journal of Cardiac Surgery 1991;6(4):476-81.

31. Ionescu MI. Long-term durability of the pericardial valve. Zeitschrift für Kardiologie 1986;75 Suppl 2:207-12.

32. Haziza F, Papouin G, Barratt-Boyes B, Christie G, Whitlock R. Tears in bioprosthetic heart valve leaflets without calcific degeneration. J Heart Valve Dis 1996;5(1):35-9.

33. Lis GJ, Rokita E, Podolec P, Pfitzner R, Dziatkowiak A, Cichocki T. Mineralization and organic phase modifications as contributory factors of accelerated degeneration in homograft aortic valves. J Heart Valve Dis 2003;12(6):741-51.

34. Stein PD, Wang CH, Riddle JM, Magilligan DJ, Jr. Leukocytes, platelets, and surface microstructure of spontaneously degenerated porcine bioprosthetic valves. J Card Surg 1988;3(3):253-61.

35. Simionescu D, Simionescu A, Deac R. Detection of remnant proteolytic activities in unimplanted glutaraldehyde-treated bovine pericardium and explanted cardiac bioprostheses. J Biomed Mater Res 1993;27(6):821-9.

36. Simionescu DT, Lovekamp JJ, Vyavahare NR. Extracellular matrix degrading enzymes are active in porcine stentless aortic bioprosthetic heart valves. J Biomed Mater Res A 2003;66(4):755-63.

37. Simionescu A, Simionescu D, Deac R. Biochemical pathways of tissue degeneration in bioprosthetic cardiac valves. The role of matrix metalloproteinases. ASAIO J 1996;42(5):M561-7.

38. Visse R, Nagase H. Matrix metalloproteinases and tissue inhibitors of metalloproteinases: structure, function, and biochemistry. Circ Res 2003;92(8):827-39.

39. Ariganello M, Labow R, Lee J. In vitro response of monocyte-derived macrophages to a decellularized pericardial biomaterial. Journal of Biomedical Materials Research Part A 2009;93(1):280-288.

40. Courtman DW, Pereira CA, Kashef V, McComb D, Lee JM, Wilson GJ. Development of a pericardial acellular matrix biomaterial: biochemical and mechanical effects of cell extraction. J Biomed Mater Res 1994;28(6):655-66.

41. Stock UA, Schenke-Layland K. Performance of decellularized xenogeneic tissue in heart valve replacement. Biomaterials 2006;27(1):1-2.

42. Vesely I. Heart valve tissue engineering. Circ Res 2005;97(8):743-55.

43. Badylak SF, Gilbert TW. Immune response to biologic scaffold materials. Semin Immunol 2008;20(2):109-16.

44. Lynn AK, Yannas IV, Bonfield W. Antigenicity and immunogenicity of collagen. J Biomed Mater Res Part B Appl Biomater 2004;71(2):343-54.

45. Baumgartner HR. Platelet interaction with collagen fibrils in flowing blood. I. Reaction of human platelets with alpha chymotrypsin-digested subendothelium. Thrombosis and Haemostasis 1977;37(1):1-16.

46. Human P, Zilla P. The possible role of immune responses in bioprosthetic heart valve failure. Journal of Heart Valve Disease 2001;10(4):460-6.

47. Zehr KJ, Yagubyan M, Connolly HM, Nelson SM, Schaff HV. Aortic root replacement with a novel decellularized cryopreserved aortic homograft: postoperative immunoreactivity and early results. J Thorac Cardiovasc Surg 2005;130(4):1010-5.

48. Vesely I, Boughner D. Analysis of the bending behaviour of porcine xenograft leaflets and of neutral aortic valve material: bending stiffness, neutral axis and shear measurements. Journal of biomechanics 1989;22(6-7):655-71.

49. Vesely I, Boughner DR, Leeson-Dietrich J. Bioprosthetic valve tissue viscoelasticity: implications on accelerated pulse duplicator testing. Ann Thorac Surg 1995;60(2 Suppl):S379-82; discussion S383.

50. Eybl E, Griesmacher A, Grimm M, Wolner E. Toxic effects of aldehydes released from fixed pericardium on bovine aortic endothelial cells. J Biomed Mater Res 1989;23(11):1355-65.

51. Cheung DT, Nimni ME. Mechanism of crosslinking of proteins by glutaraldehyde II. Reaction with monomeric and polymeric collagen. Connect Tissue Res 1982;10(2):201-16.

52. Woodroof EA. Use of glutaraldehyde and formaldehyde to process tissue heart valves. Journal of bioengineering 1978;2(1-2):1-9.

53. Cheung DT, Perelman N, Ko EC, Nimni ME. Mechanism of crosslinking of proteins by glutaraldehyde III. Reaction with collagen in tissues. Connect Tissue Res 1985;13(2):109-15.

54. Lee J, Edwards H, Pereira C, Samii S. Crosslinking of tissue-derived biomaterials in 1-ethyl-3-(3-dimethylaminopropyl)-carbodiimide EDC). J Materials Science: Materials in Medicine 1996;7(1):531-541.

55. Cheung DT, Tong D, Perelman N, Ertl D, Nimni ME. Mechanism of crosslinking of proteins by glutaraldehyde. IV: In vitro and in vivo stability of a crosslinked collagen matrix. Connect Tissue Res 1990;25(1):27-34.

56. Olde Damink LH, Dijkstra PJ, Van Luyn MJ, Van Wachem PB, Nieuwenhuis P, Feijen J. In vitro degradation of dermal sheep collagen cross-linked using a water-soluble carbodiimide. Biomaterials 1996;17(7):679-84.

57. Olde Damink LH, Dijkstra PJ, Van Luyn MJ, Van Wachem PB, Nieuwenhuis P, Feijen J. Changes in the mechanical properties of dermal sheep collagen during in vitro degradation. J Biomed Mater Res 1995;29(2):139-47.

58. Weadock KS, Olson, R.M., Silver, F.H. . Evalulation of collagen crosslinking techniques. Biomaterials Medical Devices and Artificial Organs 1983;11(4):293-318.

59. Anselme K, Petite, H., Herbage, D. . Inhibition of calcification in vivo by acyl azide cross-linking of a collagen-glycosaminoglycan sponge. Matrix 1992;12(4):264-273.

60. Pieper JS, van Wachem PB, MJA vL, Brouwer LA, Hafmans T, Veerkamp JH, van Kuppevelt TH. Attachment of glycosaminoglycans to collagenous matrices modulates the tissue response in rats. Biomaterials 2000;21(16):1689-99.

61. van Wachem PB, van Luyn, M.J., Olde Damink, L.H., Dijkstra, P.J., Feijen, J., Nieuwenhuis, P. . Biocompatibility and tissue regenerating capacity of crosslinked dermal sheep collagen. Journal of Biomedical Materials Research 1994;28(3):353-363.

62. van Wachem PB, van Luyn, M.J., Olde Damink, L.H., Dijkstra, P.J., Feijen, J., Nieuwenhuis, P. . Tissue regenerating capacity of carbodiimide-crosslinked dermal sheep collagen during repair of the abdominal wall. International Journal of Artifical Organs 1994;17(4):230-239.

63. Grabarek Z, Gergely, J. . Zero-length crosslinking procedure with the use of active esters. Analytical Biochemistry 1990;185(1):131-135.

64. Tomihata K, Ikada, Y. . Crosslinking of hyaluronic acid with water-soluble carbodiimide. Journal of Biomedical Materials Research 1997;37(2):243-251.

65. Sehgal D, Vijay, I.K. . A method for the high efficiency of water-soluble carbodiimide-mediated amidation. Analytical Biochemistry 1994;218(1):87-91.

66. Staros JV, Wright, R.W., Swingle, D.M. . Enhancement by N-hydroxysulfosuccinimide of water-soluble carbodiimide-mediated coupling reactions. Analytical Biochemistry 1986;156(1):220-222.

67. Anderson JM. Mechanisms of Inflammation and Infection With Implanted Devices. Cardiovascular Pathology 1993;2(3 Sup):S33-S41.

68. Middleton J PA, Gardner L, Schmutz C, Ashton BA. Leukocyte extravasation: chemokine transport and presentation by the endothelium. Blood 2002;100(12):3853-60.

69. Tsirogianni AK, Moutsopoulos NM, Moutsopoulos HM. Wound healing: immunological aspects. Injury 2006;37 Suppl 1:S5-12.

70. Imhof BA, Dunon D. Leukocyte migration and adhesion. Adv Immunol 1995;58:345-416.

71. Anderson JM. Multinucleated giant cells. Curr Opin Hematol 2000;7(1):40-7.

72. Ziegler-Heitbrock HW, Ulevitch RJ. CD14: cell surface receptor and differentiation marker. Immunol Today 1993;14(3):121-5.

73. Anderson JM, Rodriguez A, Chang D. Foreign body reaction to biomaterials. Semin Immunol 2008;20(2):86-100.

74. Labow R, Meek E, Matheson L, Santerre JP. Human macrophage-mediated biodegradation of polyurethanes: assessment of candidate enzyme activities. Biomaterials 2002;23(19):3969-75.

75. Labow R, Sa D, Matheson L, Dinnes DL, Santerre JP. The human macrophage response during differentiation and biodegradation on polycarbonate-based polyurethanes: dependence on hard segment chemistry. Biomaterials 2005;26(35):7357-66.

76. Matheson LA, Labow RS, Santerre JP. Biodegradation of polycarbonate-based polyurethanes by the human monocytes-derived macrophage and U937 cell systems. J Biomed Mater Res 2002;61(4):505-13.

77. Henson PM. Mechanisms of exocytosis in phagocytic inflammatory cells. Parke-Davis Award Lecture. Am J Pathol 1980;101(3):494-511.

78. Bonfield TL CE, Marchant RE, Anderson JM Cytokine and growth factor production by monocytes/macrophages on protein preadsorbed polymers. J Biomed Mater Res 1992;26(7):837-50.

79. Glaros T, Larsen M, Li L. Macrophages and fibroblasts during inflammation, tissue damage and organ injury. Front Biosci 2009;14:3988-93.

80. Mantovani A, Sica A, Sozzani S, Allavena P, Vecchi A, Locati M. The chemokine system in diverse forms of macrophage activation and polarization. Trends Immunol 2004;25(12):677-86.

81. Mosser DM. The many faces of macrophage activation. Journal of Leukocyte Biology 2003;73(2):209-12.

82. Mantovani A, Sica A, Locati M. New vistas on macrophage differentiation and activation. Eur J Immunol 2007;37(1):14-6.

83. Gordon S. Alternative activation of macrophages. Nat Rev Immunol 2003;3(1):23-35.

84. Matthews JB GT, Stone MH, Wroblewski BM, Fisher J, Ingham E. Comparison of the response of primary murine peritoneal macrophages and the U937 human histiocytic cell line to challenge with in vitro generated clinically relevant UHMWPE particles. Biomed Mater Eng 2000;10(3-4):229-40.

85. Matthews JB, Green TR, Stone MH, Wroblewski BM, Fisher J, Ingham E. Comparison of the response of three human monocytic cell lines to challenge with polyethylene particles of known size and dose. Journal of materials science Materials in medicine 2001;12(3):249-58.

86. Gao Q, Chung AS, Kao WJ. Monocytic U937 adhesion, tumor necrosis factor-alpha and interleukin-1 beta expression in response to gelatin-based networks grafted with arginine-glycine-aspartic acid and proline-histidine-serine-arginine-asparagine oligopeptides. Tissue Eng 2007;13(1):179-85.

87. Koyama Y, Norose-Toyoda K, Hirano S, Kobayashi M, Ebihara T, Someki I, Fujisaki H, Irie S. Type I collagen is a non-adhesive extracellular matrix for macrophages. Arch Histol Cytol 2000;63(1):71-9.

88. Keeley FW, J.D. Morin, and S. Vesely. Characterization of collagen from normal human sclera. 1984;39(5):533-42.

89. Ariganello MB, Labow RS, Lee JM. Response of macrophage-like U937 cells to decellularized tissue heart valve materials. J Heart Valve Dis 2009;18(2):187-97.

90. Ariganello M, Labow R, Lee J. Macrophage differentiation and polarization on a decellularized pericardial biomaterial. Submitted 2010.

91. Labow RS ME, Santerre JP. Model systems to assess the destructive potential of human neutrophils and monocyte-derived macrophages during the acute and chronic phases of inflammation. J Biomed Mater Res 2001;54(2):189-97.

92. Girardot JM, Girardot MN. Amide cross-linking: an alternative to glutaraldehyde fixation. J Heart Valve Dis 1996;5(5):518-25.

93. Khor E. Methods for the treatment of collagenous tissues for bioprostheses. Biomaterials 1997;18(2):95-105.

94. Simionescu DT, Kefalides NA. The biosynthesis of proteoglycans and interstitial collagens by bovine pericardial fibroblasts. Exp Cell Res 1991;195(1):171-6.

95. Pasquino E, Pascale S, Andreon M, Rinaldi S. Bovine Pericardium for Heart Valve Bioprostheses: In Vitro Andin Vivo Characterization of New Chemical Treatments. Journal of Materials Science: Materials in Medicine 1994.

96. Rogers PD, Stiles JK, Chapman SW, Cleary JD. Amphotericin B induces expression of genes encoding chemokines and cell adhesion molecules in the human monocytic cell line THP-1. J Infect Dis 2000;182(4):1280-3.

97. Gratzer PF, Lee JM. Control of pH alters the type of cross-linking produced by 1-ethyl-3-(3-dimethylaminopropyl)-carbodiimide (EDC) treatment of acellular matrix vascular grafts. J Biomed Mater Res 2001;58(2):172-9.

98. Matheson L, Maksym G, Santerre JP, Labow R. The functional response of U937 macrophage-like cells is modulated by extracellular matrix proteins and mechanical strain. Biochem. Cell Biol. 2006;84(5):763-73.

99. Akisaka T, Subita GP, Kawaguchi H, Shigenaga Y. Different Tartrate Sensitivity and Ph Optimum for 2 Isoenzymes of Acid-Phosphatase in Osteoclasts - an Electron-Microscopic Enzyme-Cytochemical Study. Cell and Tissue Research 1989;255(1):69-76.

100. Vanderlinde RE. Measurement of total lactate dehydrogenase activity. Ann Clin Lab Sci 1985;15(1):13-31.

101. Erfle DJ, Santerre JP, Labow RS. Lysosomal enzyme release from human neutrophils adherent to foreign material surfaces: Enhanced release of elastase activity. Cardiovascular Pathology 1997;6(6):333-340.

102. Chachra D, Gratzer PF, Pereira CA, Lee JM. Effect of applied uniaxial stress on rate and mechanical effects of cross-linking in tissue-derived biomaterials. Biomaterials 1996;17(19):1865-75.

103. Wheeler AR, Throndset WR, Whelan RJ, Leach AM, Zare RN, Liao YH, Farrell K, Manger ID, Daridon A. Microfluidic device for single-cell analysis. Anal Chem 2003;75(14):3581-6.

104. McBane JE, Santerre JP, Labow R. Effect of phorbol esters on the macrophage-mediated biodegradation of polyurethanes via protein kinase C activation and other pathways. Journal of biomaterials science Polymer edition 2009;20(4):437-53.

105. Lee JM, Pereira CA, Abdulla D, Naimark WA, Crawford I. A multi-sample denaturation temperature tester for collagenous biomaterials. Med Eng Phys 1995;17(2):115-21.

106. Schmidt CE, Baier JM. Acellular vascular tissues: natural biomaterials for tissue repair and tissue engineering. Biomaterials 2000;21(22):2215-31.

107. Kasimir MT, Rieder E, Seebacher G, Silberhumer G, Wolner E, Weigel G, Simon P. Comparison of different decellularization procedures of porcine heart valves. Int J Artif Organs 2003;26(5):421-7.

108. Yagil-Kelmer E, Kazmier P, Rahaman MN, Bal BS, Tessman RK, Estes DM. Comparison of the response of primary human blood monocytes and the

U937 human monocytic cell line to two different sizes of alumina ceramic particles. J Orthop Res 2004;22(4):832-8.

109. Dinnes DL, Santerre JP, Labow RS. Phospholipase A2 pathway association with macrophage-mediated polycarbonate-urethane biodegradation. Biomaterials 2005;26(18):3881-9.

110. Matheson LA, Santerre JP, Labow RS. Changes in macrophage function and morphology due to biomedical polyurethane surfaces undergoing biodegradation. J Cell Physiol 2004;199(1):8-19.

111. Cooke A, Olivier, RF., Edward, M. An in vivo cytotoxicity study of aldehyde-treated pig dermal collagen. Br J Exp Pathol 1983;64(1):172-176.

112. Gendler E, Gender, S., Nimni, ME. . Toxic reactions evoked by glutaraldehyde-fixed pericardium and cardiac valve tissue bioprostheses. J Biomed Mater Res 1984;18(1):727-736.

113. Matheson LA, McBane JE, Malowany JI, Santerre JP, Labow RS. Is cell culture stressful? Effects of degradable and nondegradable culture surfaces on U937 cell function. Biotechniques 2007;42(6):744, 746-50.

114. Miller KM, Anderson JM. Invitro Stimulation of Fibroblast Activity by Factors Generated from Human-Monocytes Activated by Biomedical Polymers. Journal of Biomedical Materials Research 1989;23(8):911-930.

115. Bune AJ, Hayman AR, Evans MJ, Cox TM. Mice lacking tartrate-resistant acid phosphatase (Acp 5) have disordered macrophage inflammatory responses and reduced clearance of the pathogen, Staphylococcus aureus. Immunology 2001;102(1):103-13.

116. Mosmann T. Rapid colorimetric assay for cellular growth and survival: application to proliferation and cytotoxicity assays. J Immunol Methods 1983;65(1-2):55-63.

117. Elkington PT, O'Kane, C. M., Friedland, J. S. The paradox of matrix metalloproteinases in infectious disease. Clin. Exp. Immunol. 2005;142(1):12-20.

118. Van Lint P, Libert C. Chemokine and cytokine processing by matrix metalloproteinases and its effect on leukocyte migration and inflammation. J Leukoc Biol 2007;82(6):1375-81.

119. McCawley LJ, Matrisian, L. M. . Matrix metalloproteinases: they're not just for matrix anymore! Curr. Opin. Cell Biol. 2001;13(1):534-540.

120. McQuibban GA, Gong JH, Wong JP, Wallace JL, Clark-Lewis I, Overall CM. Matrix metalloproteinase processing of monocyte chemoattractant proteins generates CC chemokine receptor antagonists with anti-inflammatory properties in vivo. Blood 2002;100(4):1160-7.

121. Parks WC, Wilson CL, López-Boado YS. Matrix metalloproteinases as modulators of inflammation and innate immunity. Nat Rev Immunol 2004;4(8):617-29.

122. Lolmede K, Campana L, Vezzoli M, Bosurgi L, Tonlorenzi R, Clementi E, Bianchi ME, Cossu G, Manfredi AA, Brunelli S and others. Inflammatory and alternatively activated human macrophages attract vessel-associated stem cells, relying on separate HMGB1- and MMP-9-dependent pathways. Journal of Leukocyte Biology 2009;85(5):779-87.

123. Jones J, Mcnally A, Chang D, Qin L, Meyerson H, Colton E, Kwon I, Matsuda T, Anderson JM. Matrix metalloproteinases and their inhibitors in the foreign body reaction on biomaterials. Journal of biomedical materials research Part A 2008;84A(1):158-166.

124. Schmidt D, Kao WJ. Monocyte activation in response to polyethylene glycol hydrogels grafted with RGD and PHSRN separated by interpositional spacers of various lengths. Journal of biomedical materials research Part A 2007;83(3):617-25.

125. Simionescu A, Simionescu, D., Deac, R. . Matrix metalloproteinases in the pathology of natural and bioprosthetic cardiac valves. Cardiovascular Pathology 1996;5(6):323-332.

126. Calero P, Jorge-Herrero E, Turnay J, Olmo N, de Lopez SI, Lizarbe MA, Maestro MM, Arenaz B, Castillo-Olivares JL. Gelatinases in soft tissue biomaterials. Analysis of different crosslinking agents. Biomaterials 2002;23(16):3473-8.

127. Chung A, Gao Q, Kao WJ. Macrophage matrix metalloproteinase-2/-9 gene and protein expression following adhesion to ECM-derived multifunctional matrices via integrin complexation. Biomaterials 2007;28(2):285-98.

128. Mertz PM DD, Stetler-Stevenson WG, Wahl LM. Interleukin 10 suppression of monocyte prostaglandin H synthase-2. Mechanism of inhibition of

prostaglandin-dependent matrix metalloproteinase production. J Biol Chem 1994;269:21322-9.

129. Schutte RJ, Parisi-Amon A, Reichert WM. Cytokine profiling using monocytes/macrophages cultured on common biomaterials with a range of surface chemistries. Journal of Biomedical Materials Research 2007;88(1):128-39.

130. Zimmerman MA RL, Raeburn CD, Selzman CH. Interleukin-10 attenuates the response to vascular injury. J Surg Res 2004;121(2):206-213.

131. Bayrak A TM, Ladhoff J, Schleicher M, Stock UA, Volk HD, Seifert M. Human immune responses to porcine xenogeneic matrices and their extracellular matrix constituents in vitro. Biomaterials 2010;31(14):3793-803.

132. Mocellin S MF, Rossi CR, Nitti D, Lise M. . The multifaceted relationship between IL-10 and adaptive immunity: putting together the pieces of a puzzle. Cytokine Growth Factor Rev 2004;15(1):61-76.

133. Jones J, Chang D, Meyerson H, Colton E, Kwon I, Matsuda T, Anderson JM. Proteomic analysis and quantification of cytokines and chemokines from biomaterial surface-adherent macrophages and foreign body giant cells. Journal of biomedical materials research Part A 2007;83(3):585-96.

134. Girardot JM, Girardot MN. Method for Fixation of Biological Tissue. U.S. Patent 5,477,536, 1995.

135. Stout RD, Suttles J. Functional plasticity of macrophages: reversible adaptation to changing microenvironments. Journal of Leukocyte Biology 2004;76(3):509-13.

136. Hübner G, Brauchle M, Smola H, Madlener M, Fässler R, Werner S. Differential regulation of pro-inflammatory cytokines during wound healing in normal and glucocorticoid-treated mice. Cytokine 1996;8(7):548-56.

137. Kao WJ. Evaluation of leukocyte adhesion on polyurethanes: the effects of shear stress and blood proteins. Biomaterials 2000;21(22):2295-303.